Connectivity of Cognitive Device-to-Device Communications Underlying Cellular Networks

Mohammad G. Khoshkholgh, Yan Zhang, *Senior Member, IEEE*, Kwang-Cheng Chen, *Fellow, IEEE*, Kang G. Shin, *Life Fellow, IEEE*, and Stein Gjessing

***Abstract*—Providing *direct* communications among a rapidly growing number of wireless devices within the coverage area of a cellular system is an attractive way of exploiting the proximity among them to enhance coverage and spectral and energy efficiency. However, such device-to-device (D2D) communications create a new type of interference in cellular systems, calling for rigorous system analysis and design to both protect mobile users (MUs) and guarantee the connectivity of devices. Motivated by the potential advantages of cognitive radio (CR) technology in detecting and exploiting underutilized spectrum, we investigate CR-assisted D2D communications in a cellular network as a viable solution for D2D communications, in which devices access the network with mixed overlay–underlay spectrum sharing. Our comprehensive analysis reveals several engineering insights useful to system design. We first derive bounds of pivotal performance metrics. For a given collision probability constraint, as the prime spectrum-sharing criterion, we also derive the maximum allowable density of devices. This captures the density of MUs and that of active macro base stations. Limited in spatial density, devices may not have connectivity among them. Nevertheless, it is shown that for the derived maximum allowable density, one should judiciously push a portion of devices into receiving mode in order to preserve the connectivity and to keep the isolation probability low. Furthermore, upper bounds on the cellular coverage probability are obtained incorporating load-based power allocation for both path-loss and fading-based cell association mechanisms, which are fairly accurate and consistent with our in-depth simulation results. Finally, implementation issues are discussed.**

***Index Terms*—Device-to-device (D2D) communications, cellular networks, coverage probability, connectivity, interference threshold constraint, collision probability constraint, percolation, spectrum sensing, stochastic geometry.**

Manuscript received October 6, 2013; revised November 13, 2013; accepted August 5, 2014. Date of publication November 11, 2014; date of current version January 30, 2015.

M. G. Khoshkholgh is with the Department of Electrical and Computer Engineering, The University of British Columbia, Vancouver, BC V6T 1Z4, Canada (e-mail: m.g.khoshkholgh@gmail.com).

Y. Zhang is with Simula Research Laboratory, Oslo, Norway; and also with the Department of Informatics, University of Oslo, Oslo, Norway (e-mail: yanzhang@simula.no).

K.-C. Chen is with the Graduate Institute of Communication Engineering, National Taiwan University, Taipei 10617, Taiwan, and was with SKKU, Korea (e-mail: ckc@ntu.edu.tw).

K. G. Shin is with the Department of Electrical Engineering and Computer Science, University of Michigan, Ann Arbor, MI 48109-2121 USA (e-mail: kgshin@eecs.umich.edu).

S. Gjessing is with the Department of Informatics, University of Oslo, Oslo, Norway; and also with Simula Research Laboratory, Oslo, Norway (e-mail: steing@ifi.uio.no).

Color versions of one or more of the figures in this paper are available online at http://ieeexplore.ieee.org.

Digital Object Identifier 10.1109/JSAC.2014.2369611

I. Introduction

A. Device-to-Device (D2D) Technologies

DEVICE-TO-DEVICE (D2D) communications in 3GPP LTE-A and future cellular networks facilitate direct communications among devices without the intervention of wireless operators and the involvement of base stations [1]. Bluetooth and WiFi-direct are examples of D2D technologies for use in unlicensed bands, but manual pairing and short range coverage have limited their functionality. Recent trends necessitate more sophisticated technologies for D2D communications possibly in cellular bands [2]–[4], incorporating the concept of cognitive networks [5] to deal with the soon-to-be-encountered spectrum-shortage problem. The goals of D2D communications include better coverage, proximity offloading, and improvement of spectral and energy efficiency. For example, it is shown that D2D communications between macro- and femto-cell users can significantly enhance the average transmission rate of MUs, particularly for those at cell edges [4]. A variety of new applications, such as home energy management [6], are envisioned as possible applications of future cellular communications. Furthermore, D2D technologies are promising for the realization of Machine-to-Machine (M2M) communications [7], [8]. Electrical appliances and smart devices could then choose a mobile phone as a hub or data aggregator for delivering hourly/daily electrical usage/requirements to a central (cloud) server via the cellular infrastructure. This way, D2D mode can play a major role in the integration of sensor networks and cellular infrastructure towards full utilization of the merits of ubiquitous monitoring, surveillance, health care, and automation [9]. Nevertheless, the need for standardization, convincing economic models, confidentiality and security measures, and clear understanding of potential performance gains, has recently triggered a flurry of new research activities to meet the industrial requirements [1].

B. Related Work and Motivation

Approaches to D2D communications are either network-assisted or assistance-free [2]. In the former, a macro base stations (MBS) actively participate in accommodating devices in uplink/downlink communications, peer discovery, resource allocation, and interference management [10], [11]. A prohibition region was suggested in [10] to protect MUs from intolerable interference imposed by devices. A new interference-management method was proposed in [11] where a device

demodulates the received interference, signal, and retransmitted version of the interference caused by the MBS. This new method is found able to reduce the outage probability. Of prominent technical challenges are mode selection—whether devices should communicate directly in D2D mode (underlaid a cellular network [3], [12], [13]) or via MBS in cellular mode—and how actively MBS should arrange new tasks. For the single cell scenario consisting of one MBS and 3 devices, proper resource allocation in network-assisted D2D has been studied [3]. Although the results are promising in boosting spectral efficiency, MBSs need to know all possible channel side information (CSI) involved not only in uplink/downlink channels but also among all devices for optimal mode selection. This dramatically increases the signalling complexity/overhead, especially in multi-cell multi-device scenarios, unless optimal resource allocation and thus expected performance improvement may not be achievable. On the other hand, the latter is more about *ad hoc* networking in cellular infrastructure[1] based on the key features of cognitive radio networks in exploring an under-utilized portion of licensed bands [15], [16]. One of its main advantages is the limited interaction between primary (cellular) and secondary or cognitive (D2D) users and is thus aligned with the main definition of D2D communications. In essence, the potential of cognitive radio for enhancing spectral efficiency is recognized, and communications are mainly managed distributively. From a deployment perspective, assistance-free D2D seems more suitable as it does not require any major upgrades/changes in the cellular infrastructure. Nevertheless, compared to the assisted D2D case, this scenario has not been investigated enough and several issues, such as interference management and D2D performance, remain to be further explored. In this paper, we focus on assistance-free D2D communications and highlight many technical aspects. Our analysis facilitates straightforward system configuration.

Route discovery in assistance-free D2D mode was investigated in [17], [16] subject to minimum required Signal to Interference plus Noise Ratio (SINR) at MBSs. The benefits of *ad hoc* D2D in reducing power consumption were identified there, while preserving the cellular outage probability. However, only a very limited number of cells were considered. Moreover, in real scenarios, we need to consider aggregated interference in D2D mode. Distribution of transmission power and SINR in assistance-free D2D mode were also analyzed in [18]. However, the impact of interference imposed on devices because of cellular communications and on cellular receivers because of D2D mode was not considered. In [15] spectrum sharing between cellular infrastructures and mobile ad hoc networks (MANET) was considered and the corresponding performances for both overlay and underlay spectrum sharing were compared. In [15], [19], [20], overlay was referred to as disjoint spectrum allocation between primary and secondary users. Overlay was then shown to outperform underlay (in the underlay spectrum sharing, both primary and secondary services simultaneously access the entire available spectrum subject to tolerable interference at the primary receivers) from the perspective of transmission capacity [15], [19]. Note that the overlay scenario is preferable but coordination among MBS and secondary users for spectrum allocation is required, and devices, however, only use a simple random access protocol rather than sophisticated cognitive radio algorithms. Unlike spectrum splitting, we focus on mixed overlay–underlay cognitive assistance-free D2D communications in which devices sense the spectrum to detect whit spaces. Note that this protocol has not been studied for general scenarios including multi-primary transceivers and multi-secondary transceivers, which is in fact the scenario of D2D mode underlying cellular networks.

It is worth noting that the benefit of agility in secondary networks is due mainly to opportunistic exploit of the surrounding wireless environment in order to detect the under-utilized portion of the spectrum [5] by adopting spectrum sensing mechanisms such as energy detection [21], [22]. Sensing is, of course, prone to inaccuracy, and the collision probability constraint (CPC) (Q, ζ) is thus suggested to control the negative effect on primary users [23]–[25]. In fact, greater interference at the primary receiver due to secondary transmissions than the predefined interference threshold constraint Q, leads to collisions between primary and secondary data that the corresponding probability needs to be kept below ζ [26]. Contrary to [15], [19], we adopt energy detection based spectrum sensing for the mixed overlay–underlay spectrum access with CPC as the spectrum sharing constraint. Moreover, in addition to the transmission capacity explored in [15], [19], other performance metrics such as isolation probability and connectivity are of paramount importance. To the best of our knowledge, connectivity in D2D mode underlying cellular communications has not been studied before. Study of connectivity provides insights into the possibility of multi-hop communications in D2D mode without cellular operators' intervention, facilitating the implementation of several applications of cognitive assistance-free D2D communications, for instance, in future smart grid M2M communications. To control distributed (perhaps renewable) energy resources, direct or indirect (via multi-hop communications and help of intermediate nodes) communication links among energy resources are required to reach a consensus (according to the designed distributed algorithms) on the required energy to be produced/released, e.g., see [27], [28]. In general, these types of algorithms converge if each energy resource has error-free communication links to at least a couple of neighbors. Furthermore, in distributed demand-side energy management [29], two-way communications should be held among users (e.g., residents) for the sake of online billing and optimal energy consumption/production. Hence, the main questions to be answered are: *Is it possible to ensure connectivity in a D2D network while devices are exposed to interference from cellular entities and operationally restricted via transmission power and/or density? What are the main design parameters and how could we design the system subject to spectrum sharing criteria and D2D network connectivity? How does D2D mode affect the cellular performance*?

[1]Note that this is different from integration of cellular and *ad hoc* relaying proposed in [14] since there *ad hoc* communication takes place in unlicensed bands.

C. Contributions and Organization of the Paper

This paper provides a new, rigorous analysis of coverage performance of a cellular network and the impact of D2D mode on it by using stochastic geometry and develops bounds on coverage probability. The stochastic geometry literature is rich, e.g., see [15], [30], [31] and references therein, and a powerful, accurate vehicle for studying cellular performance [30], [32]. However, the existing work in this area relies on the availability of complete transmission power at the MBS for tagged MUs. In reality, however, depending on cellular load and available sub-channels, some MBSs may stay silent on some sub-channels as they do not have MUs to serve, thus not contributing to inter-cell interference. Also, the portion of the available power allocated (by MBSs) to each serving MU depends on the underlying resource allocation strategy, the number of MUs in the coverage area, and the available bandwidth. Our analysis encompasses both of these cellular characteristics as well as D2D communication activities, and our bounds on the coverage performance are fairly accurate. Our analysis is general enough to incorporate the impacts of path-loss attenuation, fading, load based power allocation, and even limited cell-site for handoffs.

The key contributions of this paper are as follows.

- *Development of a site-percolation model* [33], [34] *for an upper bound of optimal transmission activity of devices that forms clusters with infinite size in a D2D network*. This model captures the power allocation in devices, spectrum sensing threshold, CPC, densities of MUs and MBSs. It shows the possibility of guaranteeing a sufficiently low isolation probability in D2D mode for practical CPC.
- *Derivation of key system design parameters*. Density of the devices, transmission activity of devices, and CPC are analytically explored using easy-to-compute formulas.
- *Comprehensive investigation of the impact of D2D mode on the cellular coverage probability*. This analysis sheds lights in selecting suitable values for CPC. These findings suggest the possibility of establishing cognitive assistance-free D2D networks in terms of cellular performance while guaranteeing connectivity in the D2D networks. They also provide a useful engineering guideline for network design.

This paper is organized as follows. Section II discusses the system model while Section III elaborates cell associations based on path loss and fading, and analyzes the coverage probability in a cellular network while considering D2D communications. The performance of a D2D network in the terms of isolation probability and connectivity is studied in Section IV. The simulation results are presented in Section V. In Section VI we discuss some implementation issues, and the paper concludes with Section VII.

II. System Model

We consider part of a wireless spectrum with bandwidth W Hz and Additive White Gaussian Noise (AWGN) with spectral power σ^2. The spectrum is originally allocated to a primary service, but it is also open for spectrum sharing with other services. The bandwidth is divided into J sub-channels indexed by w, each with bandwidth much smaller than a coherent bandwidth.

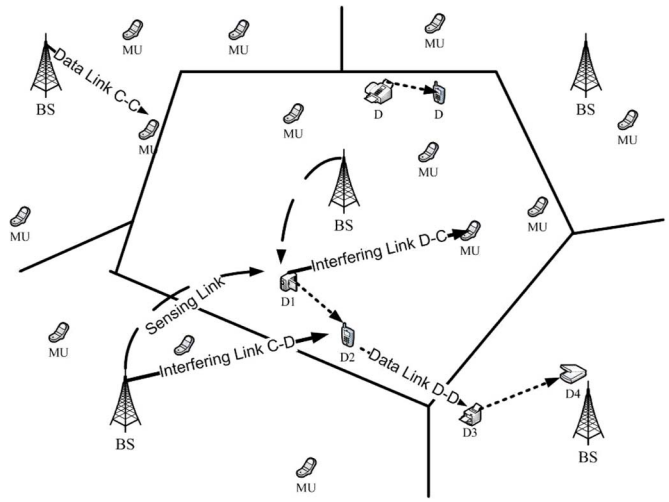

Fig. 1. A schematic diagram of D2D communications in a licensed band. D (C) refers to Device (Cellular) entities.

The primary service constitutes MBSs serving MUs in a downlink channel. The locations of MBSs are drawn according to a homogeneous (H) Poisson Point Process (PPP) $\Phi_B = \{x_i, i \in \mathbb{N}\}$ with intensity measure λ_B [15], [31], [35], which is shown to be as accurate as grid and hexagonal models and provides mathematical tractability. All MBSs in the primary system use a power-level P_T^C (C stands for Cellular) for information transmission and P_T^C for pilot transmission. Pilot signals are transmitted at the beginning of each frame for cell association. MUs measure received pilot signals and then the MBS that provides the strongest pilot will be selected for their communication. MUs are scattered geographically according to HPPP $\Phi_M = \{y_j, j \in \mathbb{N}\}$, which is independent of Φ_B, with density λ_M.

The spectrum is also available for D2D communications. Fig. 1 shows a schematic diagram of a communication scenario. Devices form a HPPP $\Phi_D = \{z_l, l \in \mathbb{N}\}$ (D stands for Device) with density λ_D. Devices selecting a sub-channel w for communication form a set $\Phi_D[w]$ that is HPPP with density $\lambda_D[w]$. For tractability we assume sub-channel selection in both cellular and D2D networks are random, unless the independency assumption is not preserved in Poisson sets. By introducing the transmission activity (probability) $a_D[w] \in [0,1]$, let $\Psi_T^D[w]$ denote the set of potential transmitters, which is a PPP with density $a_D[w]\lambda_D[w]$; likewise, potential receivers belong to the set $\Psi_R^D[w]$ with density $(1-a_D[w])\lambda_D[w]$ [36]. While MBSs broadcast information-bearing signals on sub-channel w, transmitter devices (TD) stay silent for the designated sensing window and sense the medium via an embedded energy detector or an opportunistic scheme. If the sub-channel w is declared idle for TD l, then the sub-channel is available for overlay access; otherwise, the sub-channel is busy and accessible via an underlay scheme, which we refer to as mixed overlay–underlay spectrum sharing [37]. In the overlay, TD l transmits with its maximum power, but the transmission power is limited in the underlay. Let $I^l_{C\to D}[w]$ be the imposed interference from the primary service on TD l on sub-channel w. If $I^l_{C\to D}[w]/\sigma^2 > \varepsilon^D_{th}$, where ε^D_{th} is the spectrum sensing threshold, the sub-channel w is busy and access is made based on underlay spectrum sharing. In this case, the TDs transmit at a power level P_U^D. On the

other hand, when $I^l_{C\to D}[w]/\sigma^2 \le \varepsilon^D_{th}$, the sub-channel w is idle and an overlay access will be made with transmission power $P^D_O > P^D_U$. TDs that sense the sub-channel w idle belong to the set $\Phi^D_O[w] = \{z_l \in \Phi_D[w] : I^l_{C\to D}[w]/\sigma^2 \le \varepsilon^D_{th}\}$ with density $\lambda^D_O[w] = \lambda_D[w]a_D[w]\mathbb{P}\{I_{C\to D}[w] \le \sigma^2\varepsilon^D_{th}\}$. On the other hand, TDs with underlay spectrum sharing belong to the set $\Phi^D_U[w] = \{z_l \in \Phi_D[w] : I^l_{C\to D}[w]/\sigma^2 > \varepsilon^D_{th}\}$ with intensity measure $\lambda^D_U[w] = \lambda_D[w]a_D[w]\mathbb{P}\{I_{C\to D}[w] > \sigma^2\varepsilon^D_{th}\}$. Then, $\Psi^D_T[w] = \Phi^D_U[w] \bigcup \Phi^D_O[w]$ will hold.

Here we focus on CPC as the main spectrum sharing criterion [25], [38]. The transmission activity of TDs in $\Psi^D_T[w]$ may cause intolerable interferences at MUs, which, in turn, jeopardizes the coverage performance of a cellular system. To regulate the negative impact of the devices on the coverage performance, CPC (Q,ζ) is imposed as the main spectrum sharing criteria [23], [25], [38]. Q, referred to as the interference threshold constraint, is the bearable interference level for MUs and ζ is the maximum allowable collision probability. Let $I^i_{D\to C}[w]$ be the aggregated imposed interference from TDs on MU i receiving data on sub-channel w, the *interference probability* [26] is correspondingly defined as

$$p_I = \mathbb{P}\left\{I^i_{D\to C}[w] > Q\right\}. \tag{1}$$

Then, if $I^i_{D\to C}[w] > Q$, then collision between secondary and primary data occurs, and it is necessary to enforce $p_i \le \zeta$. Note that $I^i_{D\to C}[w]$ includes interference from all TDs with both underlay and overlay spectrum access and is formulated as

$$I^i_{D\to C}[w] = \sum_{z_l \in \Phi^D_O[w]} P^D_O H^{DC}_{z_l y_i} L(z_l, y_i)^{-\alpha} + \sum_{z_l \in \Phi^D_U[w]} P^D_U H^{DC}_{z_l y_i} L(z_l, y_i)^{-\alpha}, \tag{2}$$

where $L(x,y)$ denotes the distance between a sender located at x and a receiver located at y, and $\alpha > 2$ is the path-loss exponent. Also, H^{DC}_{zy} denotes the channel power gain between device z (superscript D stands for Device) and MU y (superscript C stands for Cellular). This way, $H^{DD}_{z_1,z_2}$, H^{CD}_{xz}, and H^{CC}_{xy} are defined, by assuming that channel power gains are i.i.d. Rayleigh random variables independent of locations [31].

As one can see from Fig. 1, on each sub-channel, the interaction between cellular infrastructure and devices can be abstracted through four different interferences: $I_{C\to C}[w]$, $I_{D\to C}[w]$, $I_{C\to D}[w]$ at TDs, and $I_{C\to D}[w]$ at receiver devices (RD). Investigation of $I_{D\to C}[w]$ through the notion of interference probability reveals the impact of D2D mode on the cellular performance. However, $I_{C\to D}[w]$ indicates the spectrum availability at the TDs and the SINR qualities at the RDs. In this paper, we comprehensively analyze these four types of interferences, and appropriate metrics are then evaluated. First, coverage performance is analyzed incorporating the impact of inter-cell interference $I_{C\to C}[w]$ as well as $I_{D\to C}[w]$. To this end, we also study cell association in the cellular network. This indicates the density of active MBS, which also plays a major role in determining the availability of spectrum at TDs. For given CPC, density of devices, power allocation, and transmission activity, the relationship between D2D mode and cellular coverage by deriving upper-bounds on the coverage probability is investigated. Second, we study the density of TDs with overlay and underlay accesses by scrutinizing $I_{C\to D}[w]$ at TDs. Having the density of TDs with the overlay/underlay network structure, we can then evaluate the interference probability by examining $I_{D\to C}[w]$. Enforcing CPC, the maximum allowable density of devices is then derived. Third, adopting the site-percolation model [33], we analyze the connectivity in a D2D network by taking $I_{D\to C}[w]$ and $I_{D\to D}[w]$ at RDs into consideration. Connectivity then reveals the optimal transmission probability and random sub-channel assignment.

III. Coverage Probability in Cellular Infrastructure

We now examine the impact of D2D mode on the cellular coverage probability. In cellular communications in addition to the inter-system interference due to D2D mode, there exists inter-cell interference imposed by neighbors. Modeling and examining inter-cell interference is challenging and is affected by the cell-association policy and the resource-allocation strategy. We first need to elaborate cell association to evaluate the number of MUs served by each MBS. This is crucial in our analysis since each MBS is limited by its transmission power; the available power budget at each MBS should be shared among MUs in the associated coverage area. Here, for simplicity, we only consider an equal power allocation.

A. Cell Association

At the start of each frame, MBSs transmit pilot signals. The MUs then select the MBS with the strongest pilot. Two types of cell association are conceivable: long-term path-loss-based and short-term fading-based. In this paper, we only focus on these two broad types of cell association, although consideration of design-level aspects, such as traffic and energy efficiency, might also be useful [39], [40]. In path-loss-based cell association, MUs measure only the average power of received pilots, so the cell association may be valid for a number of frames depending on the mobility of the MUs. On the other hand, when cell association also captures the effect of fading fluctuations, for each frame a new cell association should be performed assuming that fading independently fluctuates at the start of each frame. For simplicity, we assume that the dedicated pilot channel is highly correlated with channel power gains belong to the considered part of the spectrum (with bandwidth W). In the following, we derive the load statistics for both path-loss-based and fading-based cell associations.

Theorem 1: In path-loss based cell association, $\kappa = \frac{\lambda_M}{\lambda_B}$ is the mean number of MUs in each cell.

Proof: See Appendix I.

Since pilot measurements at MUs may not be done independently, the number of MUs associated with each MBS, N, may not be Poisson r.v. In fact, by following notations presented in Appendix I, one may show that the Laplace transform of

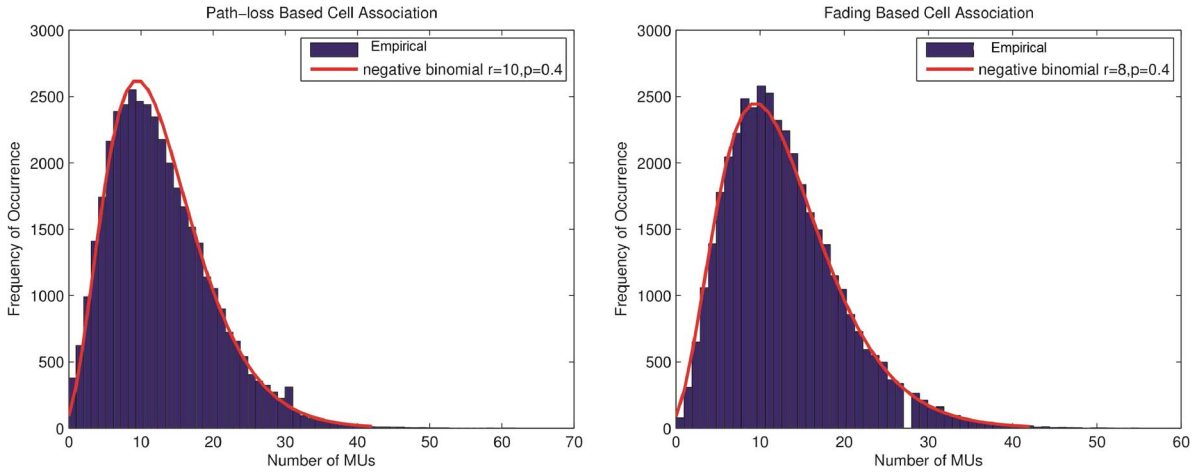

Fig. 2. Empirically obtained histograms of the number of MUs associated with each MBS in path-loss-based cell association (left) and fading-based cell association (right).

N upper-bounds the Laplace transform of a Poisson r.v. with parameter κ as

$$\begin{aligned}\mathcal{L}_N(s) &= \mathbb{E}_{\Phi_B,\Phi_M} e^{-\sum\limits_{y\in\Phi_M} s\mathbf{1}\left(L(x_i,y)^{-\alpha}>\max_{x_j\in\Phi_B/x_i} L(x_j,y)^{-\alpha}\right)} \\ &= \mathbb{E}_{\Phi_B} e^{-\lambda_M \int\limits_{\mathbb{R}^2}\left(1-e^{-s\mathbf{1}\left(y^{-\alpha}>\max_{x_j\in\Phi_B/x_i} L(x_j,y)^{-\alpha}\right)}\right)dy} \\ &= \mathbb{E}_{\Phi_B} e^{-\lambda_M(1-e^{-s})\int\limits_{\mathbb{R}^2}\mathbf{1}\left(y^{-\alpha}>\max_{x_j\in\Phi_B/x_i} L(x_j,y)^{-\alpha}\right)dy} \\ &= \sum_{n=0}^{\infty}\frac{(-\lambda_M(1-e^{-s}))^n}{n!} \\ &\quad\times \mathbb{E}_{\Phi_B}\left(\int\limits_{\mathbb{R}^2}\mathbf{1}\left(y^{-\alpha}>\max_{x_j\in\Phi_B/x_i} L(x_j,y)^{-\alpha}\right)dy\right)^n \\ &\geq \sum_{n=0}^{\infty}\frac{(-\lambda_M(1-e^{-s}))^n}{n!} \\ &\quad\times\left(\int\limits_{\mathbb{R}^2}\mathbb{E}_{\Phi_B}\mathbf{1}\left(y^{-\alpha}>\max_{x_j\in\Phi_B/x_i} L(x_j,y)^{-\alpha}\right)dy\right)^n \\ &= \sum_{n=0}^{\infty}\frac{(-\kappa(1-e^{-s}))^n}{n!}\end{aligned}$$

where we have used the convexity of function $g(x)=x^n$ for $x\geq 0$ and integer n. Calculating the Laplace transform of N is rather difficult and may not lead to a closed-form expression. On the other hand, as Fig. 2 illustrates, our simulation results indicate that random variable N acts closely to a negative binomial random variable. Unfortunately, it is challenging to estimate parameters r and p of the involved negative binomial random variable from the Laplace transform. For tractability, N is assumed to be Poisson r.v. with parameter κ. A Poisson random variable with parameter λ is, in fact, a negative binomial r.v. with parameters r and $p=\frac{\lambda}{\lambda+r}$ when $r\to\infty$. Furthermore, the simulation results in Section V confirm that this is a reasonable assumption when analyzing the performance metrics in cellular and D2D networks.

Proposition 1: The average number of MUs associated with each MBS when cell association undergoes Rayleigh fading is $\tilde{\kappa}=\frac{\lambda_M}{\lambda_B\Gamma(\alpha)}$ where $\Gamma(\alpha)=(1-\frac{2}{\alpha})\Gamma(1+\frac{2}{\alpha})$ and $\Gamma(z)=\int\limits_0^{\infty}x^{z-1}e^{-x}\,dx$.

Proof: See Appendix II.

Remark 1: Note that the approach for cell association in Theorem 1 and Proposition 1 is general enough to encompass more practically appealing scenarios. For instance, in reality, MUs are only capable of incorporating a limited number of MBSs in the cell association mechanism due mainly to complexity and hardware limitations. It may be impossible to detect very weak received pilots, so one may suggest handling a limited number of pilots, emitted from MBS in the proximity, for the sake of cell association. By introducing $\gamma_M\geq 0$, we define a set $\Phi_M^{x_i}=\{y_j\in\Phi_M : P_T^C H_{x_iy_j}^{CC} L(x_i,y_j)^{-\alpha}>\gamma_M\}$ for MUs that receive a strong enough pilot signal from MBS i. For MU y_j, we also define $\Phi_B^{y_j}=\{x_i\in\Phi_B : P_T^C H_{x_iy_j}^{CC} L(x_j,y_j)^{-\alpha}>\gamma_M\}$, indicating the MBS that provides a strong enough pilot signal for MU y_j. Following the same lines in the proof of Theorem 1 in Appendix I, we have

$$\begin{aligned}(2\pi\lambda_M)^{-1}\kappa_i(\gamma_M) &= (2\pi\lambda_M)^{-1}\mathbb{E} \\ &\quad\times\left[\sum_{y\in\Phi_M^{x_i}}\mathbf{1}\left(H_{x_iy_j}^{CC}L(x_i,y_j)^{-\alpha}>\max_{x_j\in\Phi_B^{y}/x_i} H_{x_jy_j}^{CC}L(x_j,y_j)^{-\alpha}\right)\right]\end{aligned}$$

which is equal to

$$\begin{aligned}&= \int_0^{\infty}\mathbb{E}\left[\mathbf{1}\left(H_{x_i0}^{CC}r^{-\alpha}>\max_{x_j\in\Phi_B^0/x_i} H_{x_j}^{CC}\|x_j\|^{-\alpha}\right)\right] \\ &\quad\times\mathbb{P}\left\{H_{x_i0}^{CC}r^{-\alpha}>\frac{\gamma_M}{P_P^C}\right\}r\,dr \\ &= \int_0^{\infty} e^{-2\pi\lambda_B\int_0^{\infty}\mathbb{P}\left\{H^{CC}r^{-\alpha}<H^{cc\prime}x^{-\alpha}\right\}\mathbb{P}\left\{H^{CC\prime}x^{-\alpha}>\frac{\gamma_M}{P_P^C}\right\}x\,dx} \\ &\quad\times e^{-\frac{\gamma_M}{P_P^C}r^{\alpha}}\,r\,dr \qquad (3) \\ &= \int_0^{\infty} e^{-\pi\lambda_B\Gamma\left(1+\frac{2}{\alpha}\right)\mathbb{E}_H\left[\frac{1}{Hr^{-\alpha}+\frac{\gamma_M}{P_P^C}}\right]^{\frac{2}{\alpha}}-\frac{\gamma_M}{P_P^C}r^{\alpha}}\,r\,dr. \qquad (4)\end{aligned}$$

It is easy to see that by letting $\gamma_M = 0$, (4) reduces to Proposition 1. Furthermore, increasing γ_M to ∞ results in $\kappa_i(\gamma_M) \to 0$.

Let $\|X_i\|$ be the distance between a typical MU located at the origin and MBS i provided that the MBS serves this user. In the following lemma, we derive the pdf of this random variable.

Lemma 1: In path-loss-based cell association, the pdf of r.v. $\|X_i\|$ provided that MBS i serves a typical user is $f_{\|X_i\|}(x) = 2\pi\lambda_B x e^{-\pi\lambda_B x^2}$ for $x > 0$.

Remark 2: Note that Theorem 1 and Lemma 1 are consistent with the Voronoi Tessellation prediction [30], [41]. Nevertheless, the approach developed in the proof of Theorem 1 is general and can handle more sophisticated scenarios, including fading-based cell association as presented in Lemma 2 below.

Lemma 2: When the cell-association procedure contains fading fluctuation, the pdf of random variable $\|X_i\|$ is $f_{\|X_i\|}(x) = 2\pi\lambda_B\Gamma(\alpha)x e^{-\pi\lambda_B\Gamma(\alpha)x^2}$ for $x > 0$.

Proof: See Appendix III.

Note that Lemmas 1 and 2 are general and do not depend on the Poisson assumption made on the probability mass function for random variable N. Now, we are ready to analyze the coverage probability in a cellular network.

B. Cellular Coverage Probability

We first focus on path-loss-based cell association. Due to the stationarity of the PPP, we only need to analyze the coverage probability at a typical MU located at the origin [42]. This user is in coverage if the received signal from the serving MBS is detectable. From a SINR point of view, the received SINR seen at a typical user y_0 associated with MBS i should be larger than system parameter β^C. Let sub-channel w be assigned to MU y_0, the SINR is then given by

$$\mathrm{SINR}_i[w] = \frac{P_T^C}{N_i+1}\frac{H_{x_iy_0}^{CC}L(x_i,y_0)^{-\alpha}}{I_{C\to C}^0[w]+I_{D\to C}^0[w]+\sigma^2}. \quad (5)$$

Since MBS i already serves N_i MUs, we should divide transmission power P_T^C by N_i+1 considering the typical user. Also, note that power allocation among MUs is not usually considered in formulating SINR and hence in analysis [15], [30], [31]. Thanks to the theoretical results of cell association developed in this paper, our coverage analysis covers close-to real situations accurately. In (5), $I_{C\to C}^0[w]$ denotes the inter-cell interference contribution from MBSs on sub-channel w and is formulated as

$$I_{C\to C}^0[w] = \sum_{x_j\in\hat{\Phi}_B[w]}\frac{P_T^C H_{x_jy_0}^{CC}}{N_j L(x_j,y_0)^{\alpha}}\mathbf{1}\left(\frac{L(x_j,y_0)^{-\alpha}}{L(x_i,y_0)^{-\alpha}}<1\right). \quad (6)$$

where set $\hat{\Phi}_B[w]$ with intensity measure $\hat{\lambda}_B[w]$ represents the MBSs that have MUs to serve on sub-channel w. Let $\hat{\Phi}_B = \bigcup_w \hat{\Phi}_B[w]$ denote the MBSs that have MUs to serve, i.e., $\hat{\Phi}_B = \{x_j \in \Phi_B : N_j > 0\}$. The density of set $\hat{\Phi}_B$, $\hat{\lambda}_B$, by the result of Theorem 1 and Poisson assumption, is equal to

$$\hat{\lambda}_B = \lambda_B\mathbb{P}\{N>0\} = \lambda_B(1-e^{-\kappa}). \quad (7)$$

Recall $\kappa = \lambda_M/\lambda_B$, so in light load many MBSs stay silent. Further, for large enough λ_B, $\hat{\lambda}_B \approx \lambda_M$. In the related literature it is assumed that all MBSs are always transmitting on all available sub-channels regardless of the load, while (7) indicates that depending on the load and density of MBSs, some MBSs may stay silent on *some sub-channels*, thus not contributing to inter-cell interference (6). Furthermore, (6) indicates that by increasing N_j, the received inter-cell interference at a typical MU may decrease as MBSs are limited by the power budget. Nevertheless, since increasing N_j, which happens by increasing λ_M, results in increasing $\hat{\lambda}_B$, so the reduction in strength of (6) may partially be cancelled out. We do not consider situations in which the number of MUs associated with a MBS is larger than that of available sub-channels, J. In view of $J \gg 1$, this might happen with a very small probability[2] as $\mathbb{P}\{N_i > J\} = \sum_{n=J+1}^{\infty} e^{-\kappa}\frac{\kappa^n}{n!}$ vanishes to zero.[3] In (5), $I_{D\to C}^0[w]$ represents the interference contribution from TDs that belong to $\Psi_T^D[w]$.

The coverage probability is the probability that an event that the SINR experienced by a typical user from his tagged MBS is larger than the SINR threshold β^C, and is expressed as $P_c^C = \mathbb{E}_x\mathbb{P}\{\mathrm{SINR}_x > \beta^C\}$. Unfortunately, it may not be easy to obtain this probability. In particular, random variables $I_{C\to C}^0[w]$ and $I_{D\to C}^0[w]$ are correlated since the density $\lambda_T^D[w]$ needs the evaluation of probabilities $\mathbb{P}\{I_{C\to D}^l[w] \le \sigma^2\varepsilon_{th}^D\}$ and $\mathbb{P}\{I_{C\to D}^l[w] \le \sigma^2\varepsilon_{th}^D\}$ that statistically depend on the MBSs behaviors (density, power allocation, and serving load), which also indicates the statistics of $I_{C\to C}^0[w]$. $I_{D\to C}^0[w]$ is correlated with $H_{x_iy_0}^{CC}$ as well, and hence the Laplace-transform-based approaches [30], [31] are not applicable in this case. We therefore wish to derive an upper-bound on the coverage probability, instead of the direct inspection of it.

Theorem 2: For given CPC (Q,ζ), an upper-bound on the cellular coverage probability when cell association is based only on path-loss is

$$2\pi\lambda_B\sum_{n=0}^{\infty}\frac{e^{-\kappa}\kappa^n}{n!}\int_0^{\infty} e^{-\frac{\beta^C(n+1)x^{\alpha}\sigma^2}{P_T^C}}\left(1+\zeta e^{-\frac{\beta^C(n+1)x^{\alpha}}{P_T^C}Q}\right) \times e^{-\pi\left[\hat{\lambda}_B[w]\left(\beta^C(n+1)\right)^{\frac{2}{\alpha}}F\left(\left(\beta^C(n+1)\right)^{-\frac{2}{\alpha}},\frac{\alpha}{2}\right)+\lambda_B\right]x^2}x\,dx, \quad (8)$$

where

$$F\left(\left(\beta^C(n+1)\right)^{-\frac{2}{\alpha}},\frac{\alpha}{2}\right) = \int_{r>\left(\beta^C(n+1)\right)^{-\frac{2}{\alpha}}}\mathbb{E}_{N>0}\frac{1}{1+Nr^{\frac{\alpha}{2}}}\,dr.$$

Proof: See Appendix IV.

Remark 3: For the special case of the interference-limited scenario, $\sigma^2 = 0$, and when CPC $= (0,0)$, Theorem 2 is

[2]For example, in OFDM modulation many sub-carriers are available for each coherence bandwidth.

[3]Event $\{N_i > J\}$ is actually akin to blockage in cellular communications.

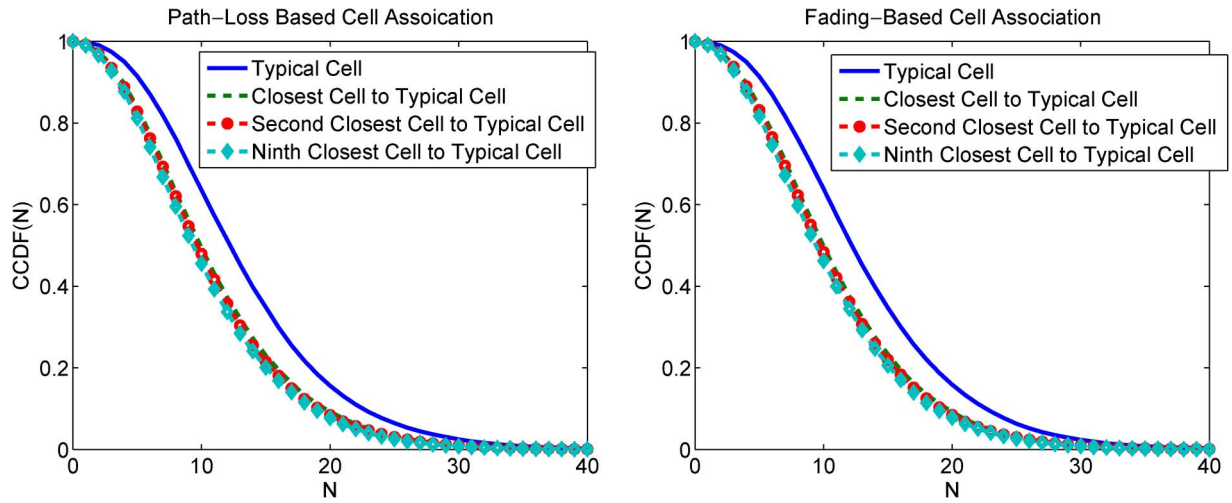

Fig. 3. Complementary Cumulative Distribution Functions (CCDF) of the load in a typical cell, the closest, the second closest, and the 9-th closest cells to the typical cell in path-loss-based cell association (left) and fading-based cell association (right) for $\lambda_B = 10^{-5}$ and $\lambda_M = 10^{-4}$.

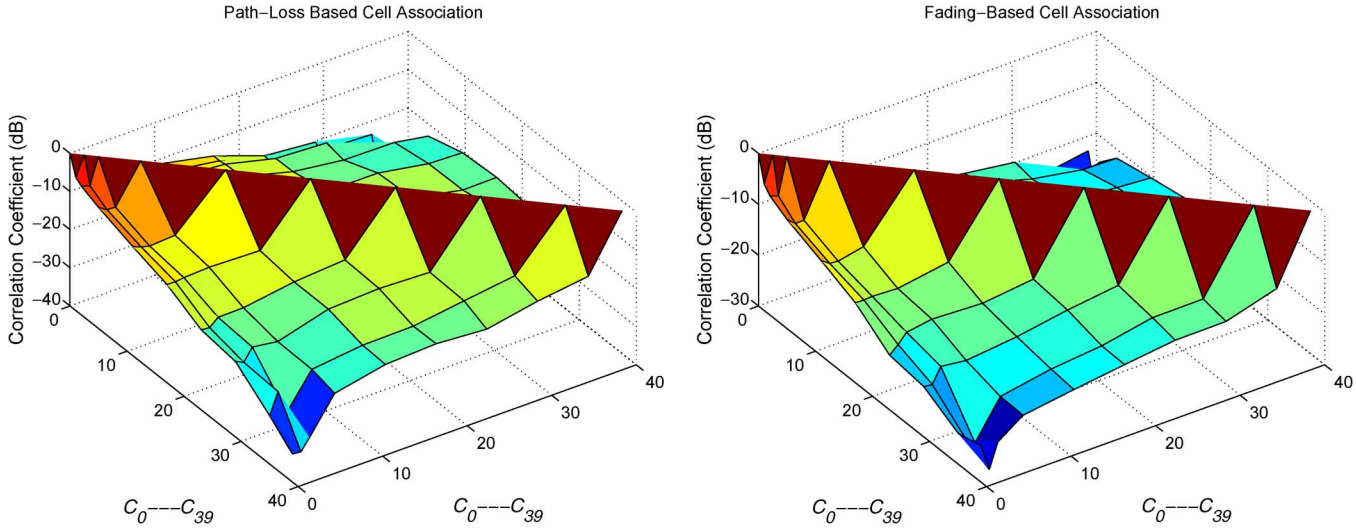

Fig. 4. Correlation coefficients among the loads in cells C_j for $j = 0, 1 \ldots, 39$. In this simulation we number cells according to the distance from the corresponding MBS to the MBS of the typical cell for $\lambda_B = 10^{-5}$ and $\lambda_M = 10^{-4}$.

simplified such that P_c^C is approximated via

$$e^{-\kappa} \sum_{n=0}^{\infty} \frac{\kappa^n}{n!} \frac{1}{1+\frac{1-e^{-\kappa}}{J} (\beta^C(n+1))^{\frac{2}{\alpha}} F\left((\beta^C(n+1))^{-\frac{2}{\alpha}}, \frac{\alpha}{2}\right)}. \quad (9)$$

As can be seen from this equation, P_c^C depends on the densities of the MBSs and the MUs through the parameter κ. P_c^C is also a non-increasing function of κ.

Remark 4: Note that (8) and $F((\beta^C(n+1))^{-\frac{2}{\alpha}}, \frac{\alpha}{2})$ involve the calculation of a series of infinite length. Our simulation results show that only the first 25 values provide accuracy. This might also be observed from a close scrutiny of Remark 3. In fact, when $n \gg 1$, the term $(\beta^C(n+1))^{\frac{2}{\alpha}} F((\beta^C(n+1))^{-\frac{2}{\alpha}}, \frac{\alpha}{2})$ rapidly converges to ∞ at a rate almost equal to $n^{2/\alpha}$.

Remark 5: In the proof of Theorem 2, we have assumed that the loads of distinct cells, N_j, are identical and independent random variables. Our simulation results indicate that the Complementary Cumulative Distribution Functions (CCDFs) of $N_j \forall\, j \neq 0$ are in fact identical (see Fig. 3). Nevertheless, the CCDF of r.v. N_0 is slightly different from the others.[4] This assumption, however, makes the mathematical development tractable and it possible to incorporate the load-based power allocation and cell-association mechanism in the study of cellular coverage probability and the D2D performance. Our simulation results confirm that the nonidentical phenomenon does not degrade the accuracy of the bound of Theorem 2. This is verifiable, especially when $(Q, \zeta) = (0, 0)$, see Fig. 5 in Section V.

Furthermore, the issue we need to discuss is the independence of $N_j \ \forall\, j = 0, 1, \ldots$. Fig. 4 indicates that there are non-negligible correlations between the loads of each cell and at least 3 nearest adjacent cells. The correlation coefficient of the

[4]In queuing systems, this phenomenon is known as Feller's paradox and states that the average time between the previous and next points in a point process is greater than the expected interval between points. In our model, knowing that an MU connects to the strongest pilot, which is equivalent to connecting to the nearest MBS in the case of path-loss-based cell association, increases the expected coverage of a typical cell [43], which in turn implies a nonidentical CCDFs of loads in the network.

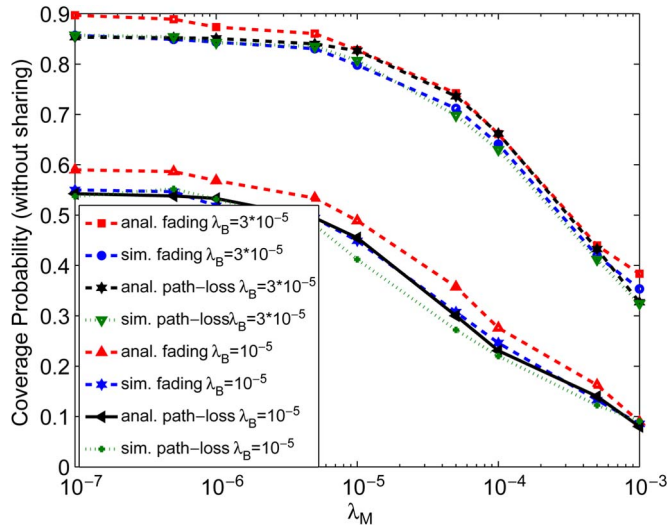

Fig. 5. Cellular coverage probability without D2D involvement. In this figure, the upper-bounds developed for both path-loss and fading based cell associations are compared via simulations.

loads between each cell and the closest cell thereof is about 0.29. However, this correlation rapidly converges to 0 for cells sufficiently far from each other. Again, our simulation results show that this dependency may not affect the accuracy of Theorem 2, as can be seen when $(Q,\zeta)=(0,0)$ in Fig. 5 in Section V.

Theorem 3: With fading-based cell association, an upper-bound on the coverage probability is

$$P_c^C \le 2\pi\lambda_B\Gamma(\alpha)e^{-\tilde{\kappa}}\sum_{n=0}^{\infty}\frac{\tilde{\kappa}^n}{n!}\int_0^{\infty}\left(\zeta e^{-\check{\lambda}_B[w]}+e^{-\check{\lambda}_B[w]+\Upsilon_Q-\Upsilon}\right)\times e^{-\pi\lambda_B\Gamma(\alpha)x^2}x\,dx, \quad (10)$$

where $\tilde{\kappa}$ is given as in Proposition 1, Υ_Q, Υ, and $\check{\lambda}_B[w]$, respectively, are

$$\Upsilon_Q = 2\pi\hat{\lambda}_B[w]\int_0^{\infty}\frac{1-e^{-\frac{(Q+\sigma^2)\beta^C(n+1)}{P_T^C}}}{1+\left(\frac{r}{x}\right)^{\alpha}}\times\left[1-e^{-\frac{(Q+\sigma^2)\beta^C(n+1)}{P_T^C}\left(1+\left(\frac{r}{x}\right)^{\alpha}\right)}\right]r\,dr, \quad (11)$$

$$\Upsilon = 2\pi\hat{\lambda}_B[w]\int_0^{\infty}\frac{1-e^{-\frac{\sigma^2\beta^C(n+1)}{P_T^C}}}{1+\left(\frac{r}{x}\right)^{\alpha}}\times\left[1-e^{-\frac{\sigma^2\beta^C(n+1)}{P_T^C}\left(1+\left(\frac{r}{x}\right)^{\alpha}\right)}\right]r\,dr, \quad (12)$$

and

$$\check{\lambda}_B[w]=\pi\hat{\lambda}_B[w]\|x\|^2\mathbb{E}\left[\left(\frac{\beta^C(n+1)}{N}\right)^{\frac{2}{\alpha}}-1\right]^+\times\int_0^{\infty}\frac{dr}{1+r^{\frac{\alpha}{2}}}+\Upsilon_Q. \quad (13)$$

Proof: See Appendix V.

Remark 6: For the special case of $(Q,\zeta)=(0,0)$ and when the system is in an interference-limited regime, the bound of Theorem 3 is simplified to

$$\sum_{n=0}^{\infty}\frac{e^{-\tilde{\kappa}}\frac{\tilde{\kappa}^n}{n!}\Gamma(\alpha)}{\Gamma(\alpha)+\frac{1-e^{-\tilde{\kappa}}}{J\alpha}\left(2\mathbb{E}\left[\left(\frac{\beta^C(n+1)}{N}\right)^{\frac{2}{\alpha}}-1\right]^+ +1\right)\int_0^{\infty}\frac{r^{\frac{2}{\alpha}-1}dr}{1+r}}. \quad (14)$$

The ratio $\tilde{\kappa}$ is a significant parameter in the coverage performance of a cellular system.

Remark 7: Theorem 3 relies on the assumption that loads in distinct cells are independent and identical. Theoretically, this is not entirely true (see Figs. 3 and 4), however the assumption causes the negligibly small inaccuracy in coverage. See Fig. 5 in Section V.

Remark 8: Theorems 2 and 3 describe the relationship between cellular coverage probability and CPC that is very important from a design point of view. In essence, we need to examine bounds (8), for the case of path-loss based cell association, for different values of CPC and derive the maximum acceptable value as described thoroughly in Section V. By doing this, we finally are able to design the D2D network without worrying about the coverage performance of the cellular system.

For a given CPC, it is then necessary to design a D2D mode such that (i) CPC is met and (ii) devices can form a connected ad hoc network. In the next section, we will show that appropriate choices of density of devices and transmission activity meet these two requirements.

IV. Connectivity in a D2D Network

In this section we show how to design a D2D network with the maximum allowable density $\lambda_D^*[w]$ of devices and the optimal transmission probability (activity) $a_D^*[w]$. The D2D mode must guarantee the satisfaction of CPC (Q,ζ) that results in a bound on $\lambda_D^*[w]$. For given system parameters, a system designer only needs to adjust the density of devices, thereby making the implementation easy and straightforward.

Devices in cognitive assistance-free D2D communications are operationally controllable via node density, and connectivity becomes a crucial performance metric, provided devices can communicate with any desired destination through multi-hop communication. Whether a TD gets isolated/disconnected or not becomes a key concern in assistance-free D2D communications. In this section we study the isolation probability and connectivity as the main metrics to evaluate the performance of cognitive assistance-free D2D communications in cellular infrastructures. Isolation might be rare but may occur at the cost of moderate to high CPC. Furthermore, we are able to suggest an upper-bound on the transmission probability a_D^* that ensures percolation in the network. This is practically important, as a careful design of transmission probability can result in formation of almost entirely connected clusters.

A. The Collision Probability Constraint (CPC)

The interference probability in (1) indicates the probability of imposing greater interference on MUs than the interference threshold Q. TDs with both overlay and underlay spectrum

access contribute to the interference. Thus, we first need to evaluate $\lambda_O^D[w]$ and $\lambda_U^D[w]$.

Proposition 2: The density of TDs with overlay spectrum access may be approximated as

$$\lambda_O^D[w] \approx \lambda_D[w] a_D[w] e^{-\pi\hat{\lambda}_B[w]\left(\frac{P_T^C}{\sigma^2\epsilon_{th}^D}\right)^{\frac{2}{\alpha}}\Gamma\left(1+\frac{2}{\alpha}\right)e^{-\kappa}\sum_{n=1}^{\infty}\frac{\kappa^n}{n!}n^{-\frac{2}{\alpha}}}. \quad (15)$$

Proof: See Appendix VI.

Knowing $\lambda_O^D[w]$, it is easy to show $\lambda_U^D[w]$ is approximated via

$$\lambda_D[w] a_D[w]\left(1-e^{-\pi\hat{\lambda}_B[w]\left(\frac{P_T^C}{\sigma^2\epsilon_{th}^D}\right)^{\frac{2}{\alpha}}\Gamma\left(1+\frac{2}{\alpha}\right)e^{-\kappa}\sum_{n=1}^{\infty}\frac{\kappa^n}{n!}n^{-\frac{2}{\alpha}}}\right). \quad (16)$$

Impacts of $\hat{\lambda}_B[w]$ and κ are notable in (15) and (16), but it may be impossible to predict how these two densities behave by changing densities of MBSs and MUs. On the other hand, our simulation results in Section V indicate that as λ_M increases, $\lambda_O^D[w]$ first decreases and then for sufficiently high λ_M, starts increasing. For a populated cellular network, devices frequently find sub-channels idle. This is somewhat surprising, but intuitively makes sense noticing the imposed interference at the TD l because of the transmission activity of active MBSs, i.e.,

$$I_{C\to D}^l[w] = \sum_{x_j\in\hat{\Phi}_B[w]} \frac{P_T^C}{N_j} H_{x_j z_l}^{CD} L(x_j, z_l)^{-\alpha}. \quad (17)$$

MBSs are sharing the available power across MUs in the corresponding coverage area. Hence, for sufficiently heavy load in the cellular system the allocated power at each MBS on given sub-channel w, and consequently accumulated interference at TDs, decreases by increasing the density of MUs. Further, note that although (15) and (16) are the estimates of $\lambda_O^D[w]$ and $\lambda_U^D[w]$, our simulations indicate that such estimations are fairly accurate, and hence they may be treated as true densities.

Let us proceed to obtain $\lambda_D^*[w]$. To this end, we set $p_I = \mathbb{P}\{I_{D\to C}^0[w] > Q\} = \zeta$. CPC also indicates devices' opportunities for spectrum access. With the virtue of near-field approximation [15], [44], we are able to provide a precise approximation of the interference probability. As a result, $\lambda_D^*[w]$ should satisfy $\exp\{-\pi\lambda_U^D[w]\Gamma(1+\frac{2}{\alpha})(\frac{Q}{P_U^D})^{-\frac{2}{\alpha}}\}\exp\{-\pi\lambda_O^D[w]\Gamma(1+\frac{2}{\alpha})(\frac{Q}{P_O^D})^{-\frac{2}{\alpha}}\} = 1-\zeta$, or equivalently, $\lambda_U^D[w]P_U^{D\,\frac{2}{\alpha}} + \lambda_O^D[w]P_O^{D\,\frac{2}{\alpha}} = \frac{Q^{\frac{2}{\alpha}}\ln\frac{1}{1-\zeta}}{\Gamma(1+\frac{2}{\alpha})}$. Thus, substituting (15) and (16), we obtain $\lambda_D^*[w]$ as:

$$\lambda_D^*[w] = \frac{Q^{\frac{2}{\alpha}}\ln\frac{1}{1-\zeta}}{a_D[w]\Gamma\left(1+\frac{2}{\alpha}\right)} \frac{1}{P_U^{D\,\frac{2}{\alpha}} + \left(P_O^{D\,\frac{2}{\alpha}} - P_U^{D\,\frac{2}{\alpha}}\right)e^{-\vartheta}} \quad (18)$$

where $\vartheta = \pi\hat{\lambda}_B[w](\frac{P_T^C}{\sigma^2\epsilon_{th}^D})^{\frac{2}{\alpha}}\Gamma(1+\frac{2}{\alpha})e^{-\kappa}\sum_{n=1}^{\infty}\frac{\kappa^n}{n!}n^{-\frac{2}{\alpha}}$.

Remark 9: Under $\lambda_D^*[w]$, underlay spectrum sharing outperforms mixed overlay–underlay spectrum sharing because (18) is always smaller than $\frac{Q^{\frac{2}{\alpha}}\ln\frac{1}{1-\zeta}}{a_D[w]\Gamma(1+\frac{2}{\alpha})}(P_U^{D\,\frac{2}{\alpha}}(1-e^{-\vartheta}))^{-1}$, which is the maximum allowable density of devices when the spectrum sharing is underlay. Furthermore, overlay spectrum sharing outperforms mixed overlay–underlay if $P_U^D > (1-e^{-\vartheta})^{\frac{\alpha}{2}}$. If $P_O^D < (e^{\vartheta}-1)^{\frac{\alpha}{2}}P_U^D$, overlay is also superior to the underlay. That is consistent with the intuition that the lower the transmission powers, the higher the maximum permissible density of devices.

We can see that $\lambda_D^*[w]$ incorporates major system parameters, especially the density of MUs and MBS as well as CPC. Hence, using (18), a fulfilling interaction between the D2D mode and the cellular requirement is guaranteed. Whenever the density of devices is lower than $\lambda_D^*[w]$, the D2D mode is transparent to the cellular network. This makes the configuration of a D2D network very straightforward and also flexible for the main system parameters, such as the density of MUs and MBSs, and the CPC.

B. Connectivity in the D2D Network

In the previous subsection, we derived an upper-bound on the density of devices. This permissible density keeps the D2D network operationally transparent to the cellular network, however devices may inevitably end up in isolation if transmission activity chooses haphazardly. We investigate the D2D network performance from a percolation perspective in order to derive the appropriate transmission activity that ensures connectivity in D2D mode with limited density. Our analysis provides instructive guidelines, with which one can judiciously adjust the transmission activity to preserve the connectivity in D2D mode.

A primary approach to understanding connectivity in wireless communications is to use the site-percolation model. This model can successfully predict the necessary condition for the network to blow up, or be fully connected. When the network percolates, it contains clusters of infinite size, so each node can reach the other nodes via multi-hop communication [33], [34]. To study the connectivity in a D2D network, we first derive the isolation probability that prohibits multi-hop communication. The lower the isolation probability, the higher the likelihood of reaching the destination via multi-hop communication.

Theorem 4: Let β^D be the SINR threshold at the RDs, a lower bound on the isolation probability on sub-channel w is $e^{-\delta[w]}$ where $\delta[w]$ is the mean degree of a typical TD and is equal to $\delta[w] = \frac{1-a_D[w]}{a_D[w]}(T_U[w]+T_O[w])$ where

$$T_U[w] = 2\pi\lambda_U^{D^*}[w]\int_0^{\infty} e^{-\frac{\beta^D r^\alpha}{P_U^D}\sigma^2} e^{-\vartheta\left(\frac{\beta^D\sigma^2\epsilon_{th}^D}{P_U^D}\right)^{\frac{2}{\alpha}} r^2} r\,dr, \quad (19)$$

$$T_O[w] = 2\pi\lambda_O^{D^*}[w]\int_0^{\infty} e^{-\frac{\beta^D r^\alpha}{P_O^D}\sigma^2} e^{-\vartheta\left(\frac{\beta^D\sigma^2\epsilon_{th}^D}{P_O^D}\right)^{\frac{2}{\alpha}} r^2} r\,dr, \quad (20)$$

and $\vartheta = \pi\hat{\lambda}_B[w](\frac{P_T^C}{\sigma^2\epsilon_{th}^D})^{\frac{2}{\alpha}}\Gamma(1+\frac{2}{\alpha})e^{-\kappa}\sum_{n=1}^{\infty}\frac{\kappa^n}{n!}n^{-\frac{2}{\alpha}}$. Furthermore,

$$\lambda_U^{D^*}[w] \approx \frac{Q^{\frac{2}{\alpha}}\ln\frac{1}{1-\zeta}}{\Gamma\left(1+\frac{2}{\alpha}\right)} \frac{1-e^{-\vartheta}}{P_U^{D\,\frac{2}{\alpha}} + \left(P_O^{D\,\frac{2}{\alpha}} - P_U^{D\,\frac{2}{\alpha}}\right)e^{-\vartheta}}, \quad (21)$$

$$\lambda_O^{D^*}[w] \approx \frac{Q^{\frac{2}{\alpha}}\ln\frac{1}{1-\zeta}}{\Gamma\left(1+\frac{2}{\alpha}\right)} \frac{e^{-\vartheta}}{P_U^{D\,\frac{2}{\alpha}} + \left(P_O^{D\,\frac{2}{\alpha}} - P_U^{D\,\frac{2}{\alpha}}\right)e^{-\vartheta}}. \quad (22)$$

Proof: See Appendix VII.

$\frac{1-a_D[w]}{a_D[w]}T_U[w]$ ($\frac{1-a_D[w]}{a_D[w]}T_O[w]$) indicates the out-degree[5] of a TD if the access is underlay (overlay). Further, $\lambda_U^{D^*}[w]/a_D[w]$ ($\lambda_O^{D^*}[w]/a_D[w]$) is the permissible density of devices with underlay (overlay) access. Note that the lower $\lambda_U^{D^*}[w]/a_D[w]$ and or $\lambda_O^{D^*}[w]/a_D[w]$ is, the lower out-degree is, and the higher isolation probability is.

Remark 10: Mixed overlay–underlay spectrum sharing always results in a lower isolation probability than both overlay and underlay. For the interference-limited scenario, Theorem 4 could be simplified to $T_U[w] = \frac{\pi\lambda_U^{D^*}[w]}{\vartheta}(\frac{\beta^D\sigma^2\varepsilon_{th}^D}{P_U^D})^{-\frac{2}{\alpha}}$, $T_O[w] = \frac{\pi\lambda_O^{D^*}[w]}{\vartheta}(\frac{\beta^D\sigma^2\varepsilon_{th}^D}{P_O^D})^{-\frac{2}{\alpha}}$. In this regime, underlay spectrum sharing results in a smaller isolation probability than overlay if $P_O^D < (e^{\vartheta}-1)^{\frac{\alpha}{2}}P_U^D$. This is consistent with our intuition that the larger the transmission power, the lower the isolation probability.

Remark 11: Note that Theorem 4 provides a lower bound of the isolation probability. This is mainly because, as in [33], we ignore the interference contribution from the TDs. It is challenging to incorporate this interference because of the dependency between the cellular contribution and the TDs' contribution on the imposed interference in an RD. Nevertheless, since we are seeking the availability of a sufficiently low isolation probability, this estimate may not hurt the accuracy of the results. Assuming that $I_{D\to D}^0$ and $I_{C\to D}^0$ are independent, we can make a more realistic approximation of the isolation probability. Here, $I_{D\to D}^i[w] = \sum_{z_l\in\Phi_O^D[w]} P_O^D H_{z_l y_i}^{DD} L(z_l,y_i)^{-\alpha_D} + \sum_{z_l\in\Phi_U^D[w]} P_U^D H_{z_l y_i}^{DD} L(z_l,y_i)^{-\alpha_D}$, where we consider a different path-loss exponent α_D for generality. Incorporating $I_{D\to D}^0$ does not alter the results of Theorem 4 (and thus Theorem 5), if $T_U[w]$ and $T_O[w]$ are updated appropriately. In such a scenario, $T_U[w]$ is

$$2\pi\lambda_U^{D^*}[w]\int_0^\infty e^{-\frac{\beta^D r^{\alpha_D}}{P_U^D}\sigma^2}\left[e^{-\vartheta\left(\frac{\beta^D\sigma^2\varepsilon_{th}^D}{P_U^D}\right)^{\frac{2}{\alpha}} r^{\frac{2\alpha_D}{\alpha}}} + e^{-\pi\beta_D^{\frac{2}{\alpha_D}}\Gamma\left(1+\frac{2}{\alpha_D}\right)a_D[w]\left(\lambda_U^{D^*}[w]+\lambda_O^{D^*}[w]\left(\frac{P_O^D}{P_U^D}\right)^{\frac{2}{\alpha_D}}\right)r^2}\right] r\,dr. \quad (23)$$

A similar formulation can also be suggested for $T_O[w]$.

Theorem 4 relates the isolation probability to cellular parameters, such as κ and the density of active MBSs. Furthermore, the impact of overlay/underlay power transmission, the sensing threshold, the CPC, and the maximum density of devices are clearly captured.

In the above discussion, we see the impact of transmission activity on the isolation probability. A natural question that may arise is the possibility to tune transmission activity while considering the satisfaction of the CPC as well as the preservation of connectivity in the D2D network. We call this transmission activity the *optimal transmission activity* $a_D^*[w]$. In the following Theorem, we derive an upper-bound on $a_D^*[w]$.

Theorem 5: An upper-bound on the optimal access probability $a_D^*[w]$ that ensures the necessary condition for percolation is $(1-\frac{1}{T_U[w]+T_O[w]})^+$ where $T_U[w]$ and $T_O[w]$ are given in Theorem 4.

Proof: See Appendix VIII.

Theorem 5 provides a straightforward configuration of D2D mode. It is only necessary to calculate $T_U[w]$ and $T_O[w]$, which are functions of κ, the density of active MBSs, the overlay/underlay power transmission, the sensing threshold, the CPC, and the maximum density of devices. The percolation is then guaranteed in the D2D network. Further, having the maximum transmission probability as the performance metric, the statements of Remarks 14 and 15 remain valid.

V. Evaluation Results

In this section we present some simulation results to delineate the interaction between cellular and D2D networks. Finally, we will investigate the isolation probability and the connectivity, confirming the possibility of establishing a cognitive assistance-free D2D mode. For this, we have 100 000 realizations of the network and in each realization MBSs, MUs, and devices are randomly scattered in a circular region with radius 7000 units. We are also interested in the accuracy of coverage bounds and the appropriate range of CPC. Our simulation parameters are set as: path-loss exponent $\alpha = 4$, number of sub-channels $J = 100$, pilot power $P_T^C = 30$ Watts, transmission power at MBS $P_c^T = 50$ Watts, density of devices $\lambda_D = 10^{-2}$, overlay transmission power $P_O^D = 0.5$ Watts, underlay transmission power $P_U^D = 0.1$ Watts, sensing threshold $\varepsilon_{th} = 10$, CPC $(Q,\zeta) = (\sigma^2, 0.05)$, and $\sigma^2 = 10^{-13}$ Watts.

A. Coverage Probability

Fig. 5 shows the coverage probability for a cellular system without D2D mode. In this case, Theorems 2 and 3 closely follow the simulation results. This figure also indicates that fading-based cell association does not offer any visible enhancement in coverage probability compared to the path-loss-based cell association. We would also like to point out that by increasing the load, the coverage probability decreases. It might partially be due to the fact that power allocated to each MU decreases the strength of the received signal compared to the interference. As to (6), the received interference might also be reduced (we will present more obvious evidences on this when we study the density of TDs with overlay and/or underlay spectrum access in Fig. 9) due to the reduction of allocated power on each sub-channel. But the observed reduction in the signal strength can cancel the impact of reduction in interference. Increasing the density of MBSs can improve the coverage performance due mainly to strengthening the transmission signals, as MBSs have a smaller number of MUs to serve.

Fig. 5 exhibits some interesting results on the accuracy of the bounds provided in Theorems 2 and 3. As also mentioned in Remarks 5 and 7, we assume the loads of cells to be independent and identical in deriving these bounds. Fig. 5 confirms that such an assumption does not harm the accuracy of the bounds.

[5]The average number of RDs that each TD have reliable communication link with is defined as out-degree.

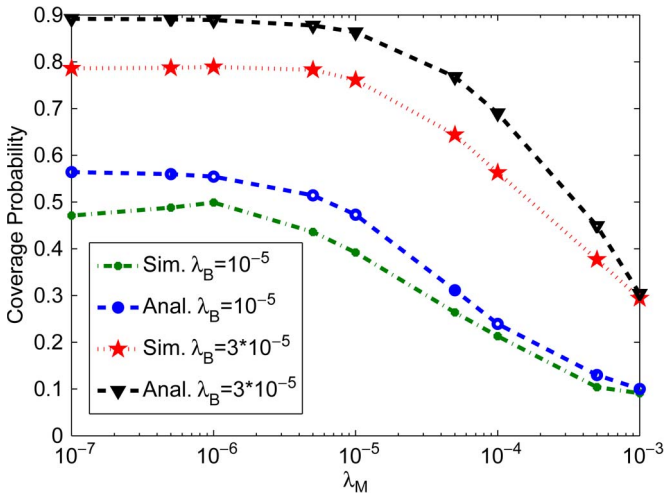

Fig. 6. Coverage probability versus λ_M when D2D mode is allowed and cell association is based on path-loss.

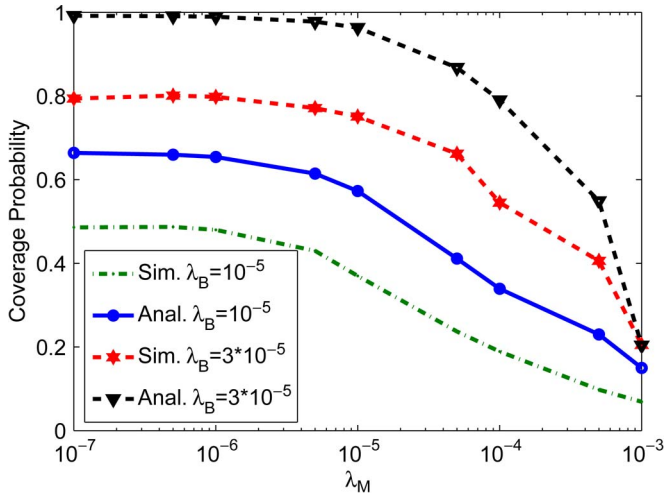

Fig. 8. Coverage probability versus λ_M when D2D mode is allowed and cell association is done based on fading.

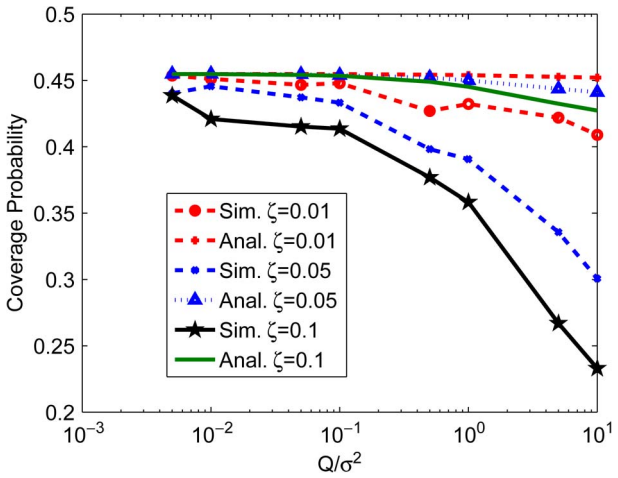

Fig. 7. Coverage probability versus interference threshold constraint for different values of ζ.

Fig. 6 depicts the coverage probability with D2D impact and path-loss-based cell association. Fig. 6 shows that using (18), Theorem 2 can actually follow the trend observed in the simulation, but in such a case, the bound is slightly looser than the case without spectrum sharing in Fig. 5. Furthermore, a close examination reveals that the coverage probability, compared to Fig. 5, is reduced (almost 5%), which is a direct impact on D2D communication.

Fig. 7 also shows the coverage probability obtained from the simulation and Theorem 2 for different values of CPC to help understand the gap between simulation and analysis. Theorem 2 is found not accurate for sufficiently large CPCs, but the bound is acceptably accurate for practical CPC, e.g., $\zeta < 0.05$ and $Q \lessapprox \sigma^2$. Moreover, the larger the CPC, the lower the coverage probability. Thus, depending on the cellular performance requirement, the designer should adjust CPC accordingly.

As Fig. 8 shows, the upper-bound developed in Theorem 3 for the fading-based cell association is looser than the simulation results. The bound is also looser than that in Fig. 6, calling for the development of a tighter bound in this case.

For fading-based cell association, the developed bound then may not be tight enough for finding an appropriate CPC. From Figs. 6 and 8, we notice that the simulation results in both path-loss-based and fading-based associations are close enough, so we may use Theorem 2 to derive CPC for the case of fading-based cell associations.

It is noteworthy that although here we only focus on assistance-free D2D communications, Fig. 6 also indicates some interesting aspects of network- assisted D2D communications, where devices could also receive/send data via downlink channels. For example, assume $\lambda_B = 3 \times 10^{-5}$ and the cellular load is not heavy, e.g., $\lambda_M = 10^{-5}$. If coverage performance 0.7 is acceptable in the primary service, which is equivalent to the cell load $\lambda_M = 5 \times 10^{-5}$, then MBSs are able to provide assistance to devices with density $\lambda_D - \lambda_D^* = 4 \times 10^{-5}$ (as we have already assigned devices with density λ_D^* for assistance-free mode). This implies that depending on the cellular load, MBSs can adaptively provide network assistance for devices without jeopardizing the required coverage performance.

B. D2D Connectivity

Fig. 9 shows the density of devices with overlay access. Intuitively, in case of low load in the cellular infrastructure, a small λ_M, many devices will sense the spectrum as idle, so $\lambda_D^O[w]$ is large. Completely opposite to our intuition, it is observed that for large enough λ_M, $\lambda_O^D[w]$ starts to increase, and thus, in case of dense load in the cellular network, devices find the spectrum fairly under-utilized again. We believe that this is because of the swift reduction of available power at MBSs for each MU. This may also indicate some clues regarding the observed high outage in Fig. 5 in a heavy load regime. It is observed that as the spectrum sensing threshold, ε_{th}, increases, $\lambda_D^O[w]$ decreases.

Fig. 10 shows the interference probability versus λ_D. Aligned with our intuition, the higher the density of devices, the larger the interference probability. Furthermore, the interference probability is reduced by increasing Q. Note that our analysis can accurately predict the real trends.

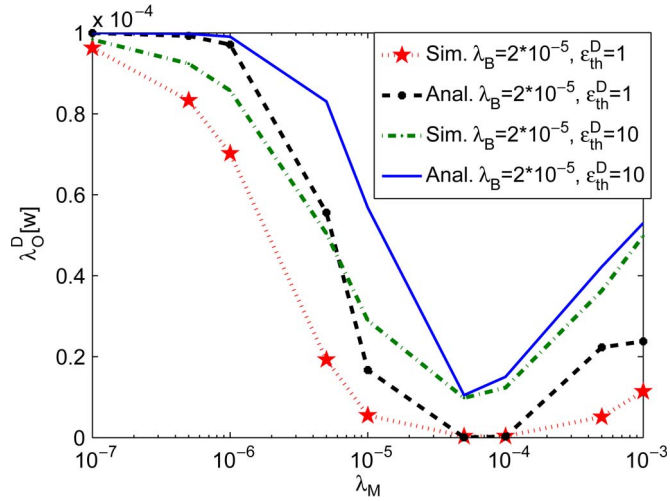

Fig. 9. $\lambda_O^D[w]$ versus λ_M.

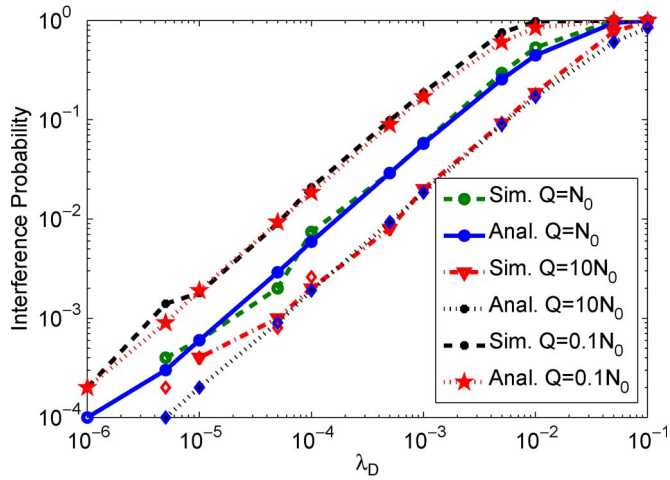

Fig. 10. The interference probability constraint versus λ_D.

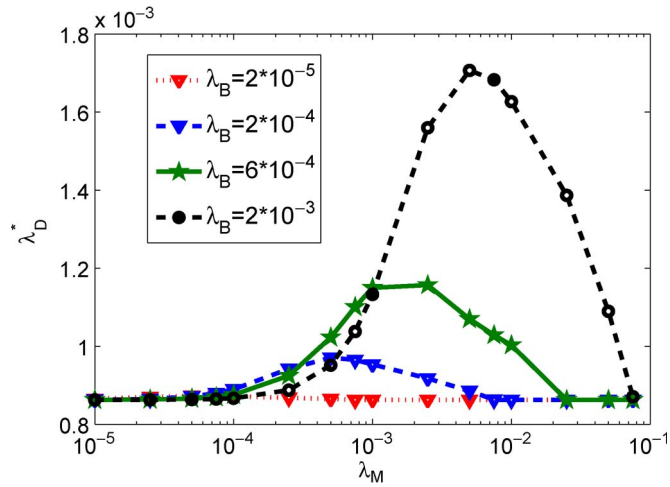

Fig. 11. λ_D^* versus λ_M for different values of λ_B.

Fig. 11 illustrates the behavior of the maximum permissible density of devices λ_D^* versus the density of MBS and MUs. As one can see, the greater the density of MBSs, the greater the density of devices. Moreover, for sufficiently small and large density of MUs, the density of MBSs does not have any impact on the density of devices since many devices find the spectrum idle. For given λ_B there is a peak in the value of λ_D^* when the density of the MUs is changed. We will use this behavior to formulate guidelines in Section VI for implementation of D2D communications in cellular bands.

Fig. 12 illustrates the isolation probability versus Q/σ^2 and transmission probability. The higher the CPC, the lower isolation probability. This is because λ_D^* is an increasing function of CPC. Furthermore, for low enough transmission activity a_D, a TD rarely ends up in isolation regardless of any CPC. In fact, forcing many devices to be in receiving mode will limit isolation incidents. This figure also shows that for moderate transmission activity and practically acceptable CPC, e.g., $\zeta < 0.05$ and $Q \lessapprox \sigma^2$, cognitive assistance-free D2D communications can guarantee a low isolation probability.

Fig. 13 depicts $a_D^*[w]$ versus λ_M and λ_B. It shows that for very low load and low MBS's density, $a_D^*[w] \approx 1$. Thus, a D2D network will percolate even if the density of TDs is high. Here, $a_D^*[w]$ is an upper-bound on the optimal transmission activity due to the ignorance of mutual interference among devices. As the load of MUs increases, we need to push more devices into receiving mode to preserve percolation. Furthermore, when the load in the cellular network is low, increasing λ_B may not affect the percolation and thus high $a_D^*[w]$ can still preserve connectivity.

Finally, Fig. 14 illustrates the impact of path-loss exponent α_D introduced in Remark 11 and the SINR threshold β^D on the isolation probability and the optimal transmission probability when the contribution from the device's interference is also incorporated. As α_D increases, the isolation probability increases as a by-product of the severe signal attenuation of high path-loss exponent. This results in a very low isolation probability (i.e., guaranteeing connectivity). On the other hand, modulation mechanisms such as CDMA can definitely compensate this phenomenon. Unfortunately, for a very high path-loss exponent, even a very low SINR threshold is not effective, thus calling for more sophisticated signal processing mechanisms such as beamforming and/or MAC scheduling.

VI. Discussion on Implementation

This section addresses the design issues of the D2D network based on the developed analysis in this paper. The central objective is the connectivity of assistance-free D2D network under the preservation of the coverage performance in cellular system. Although the analysis of this paper covers only the assistance-free D2D mode, the proposed implementation guideline covers the assistance-based D2D mode too. Suppose (i) system parameters including λ_B are fixed and given, and (ii) we need to design a D2D system for the operating point λ_M^* and λ_D^{**}. We first fix the transmission probability a_D. From Fig. 11, for given λ_B, there is a value of λ_M^* that makes the permissible density λ_D^* reach its peak, denoted by λ_D^{**}. We write $\lambda_D^*(a_D, \lambda_M)$ to express dependency on the arguments, whenever necessary. We propose a procedure to assign devices with λ_D^{**} to the assistance-free D2D communications and devices

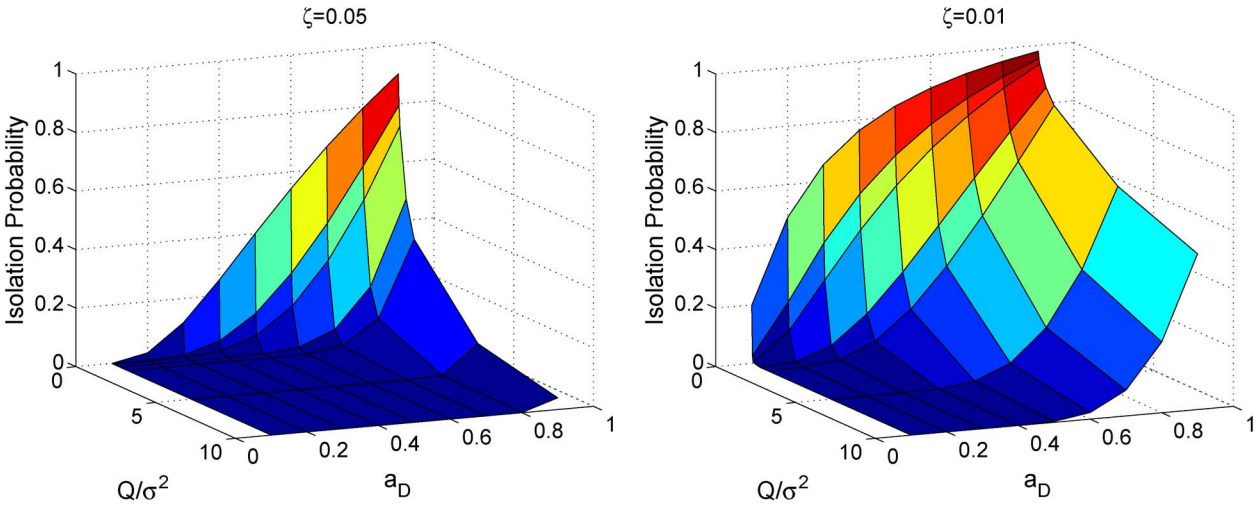

Fig. 12. Isolation probability versus transmission activity a_D and Q/σ^2.

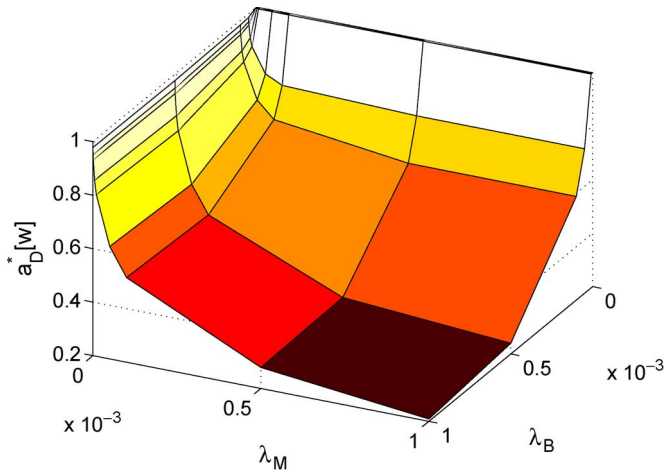

Fig. 13. An upper-bound on $a_D^*[w]$ versus λ_M and λ_B.

with density $\tilde{\lambda}_M = \max\{\lambda_M^* - \lambda_M, 0\}$ to assistance-based D2D communications. We propose the following steps.

1) For given density of MUs, λ_M, and CPC (Q,ζ), derive λ_D^* in (18).
2) Obtain λ_M^* as $\lambda_M^* = \arg\max_\mu \lambda_D^*(a_D,\mu)$.
3) Obtain $\lambda_D^{**} = \lambda_D^*(a_D,\lambda_M^*)$ that is the maximum allowable density of assistance-free devices when the density of MUs is λ_M^*.
4) For given density λ_M, we define $\tilde{\lambda}_M$ as $\tilde{\lambda}_M = \max\{\lambda_M^* - \lambda_M, 0\}$.
5) Assign a set of devices with density $\tilde{\lambda}_M$ to be a part of the MUs. These devices could communicate according to assistance-based D2D communications via the cellular infrastructure. Check the coverage performance of the cellular system with load λ_M^* and CPC (Q,ζ). If it is satisfactory, then go to step 6, else find a new CPC (Q^*,ζ^*) that meets the coverage requirements.
6) Set $(Q,\zeta) = (Q^*,\zeta^*)$ and go to step 1.
7) Calculate a_D^* for total cellular load λ_M^*. This value guarantees the connectivity among assistance-free devices with density λ_D^{**}.
8) Now, go back and repeat steps 1 to 6 by replacing a_D with a_D^* and then terminate the procedure after performing step 6.

There is also room for assigning devices to either assistance-free D2D mode or assistance-based D2D mode. One possible approach is to assign devices with severe delay penalties to assistance-based D2D communications, provided the density does not violate $\tilde{\lambda}_M$. On the other hand, devices that are falling in cell edges and have elastic data for transmission could be assigned for assistance-free D2D communications. In this case, according to the developed cognitive assistance-free D2D communications, the data will be transported via multi-hop communications toward the devices that are either the final destinations or close enough to a MBS for assistance-based D2D mode. This is important for interference management in cellular communications as long distance communication between devices would be split in many short distance communications.

Another policy in assigning the devices to either assistance-based or assistance-free D2D communications can be managed with the cellular signaling mechanism. Devices that can detect at least $L \in \mathbb{N}$ different pilot signals, where L is a system design parameter, could be used for assistance-based D2D communications. Since pilot detection depends mainly on the strength of the received pilot and threshold γ_M, according to Remark 1, the designer needs to choose L such that $\mathbb{P}\{\texttt{Detecting } L \texttt{ Pilots}\} = \frac{\tilde{\lambda}_M}{\tilde{\lambda}_M + \lambda_D^{**}}$. The remaining devices will be assigned to assistance-free D2D communications.

VII. Conclusion

We proposed mixed overlay–underlay spectrum sharing for assistance-free D2D mode in cellular communication systems. Many important aspects of these systems have been analyzed and appropriate performance metrics have been derived. Guidelines for designing key system parameters have been presented. In conclusion, this paper provided:

1) A thorough analysis to accurately capture the interactions between devices and cellular infrastructures using tools from PPP and stochastic geometry.

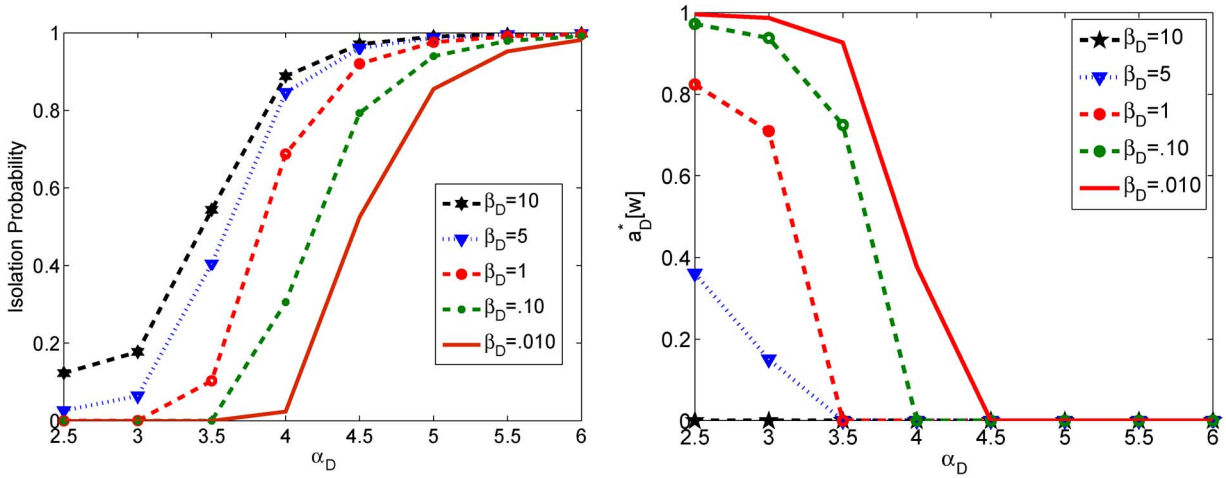

Fig. 14. Isolation probability (left) and optimal transmission probability (right) versus α_D for different values of β_D with considering the impact of the devices's interference.

2) New insights on modeling and analysis of cell-association mechanisms, load characterization, and power allocation. Different cell-association mechanisms, such as path-loss, fading, and threshold-based cell associations, have been analyzed. We further observed that loads of distinct cells are almost identical and independent. This allowed us to study the load-based power allocation in cellular systems which is new and led us to more accurate interference characterization and coverage analysis in cellular systems as well as opportunity detection in cognitive D2D systems. Finally, we derived accurate upper bounds of the coverage probability of cellular systems, highlighting the importance of the ratio among the density of MUs and MBSs, power allocation, and the impact of silent MBSs.
3) Decoupling the design of the assistance-free D2D network from cellular systems by choosing permissable CPC values that preserve coverage performance of the cellular system. Using the value of CPC, we derived the maximum permissable density and the maximum transmission probability of devices that preserve connectivity and low isolation probability in D2D mode.
4) Implementation guidelines. Accurate system design is made possible to accommodate not only assistance-free D2D communications but also assistance-based D2D communications. Some insights in assigning devices to these two groups were also discussed.

APPENDIX I

Proof of Theorem 1: We first note that mobile y will connect to MBS i if the observed pilot strength is the strongest among all measured pilots, i.e., $P_T^C L(x_i,y)^{-\alpha} > \max_{x_j\in\Phi_B/x_i} P_T^C L(x_j,y)^{-\alpha}$. Let $\mathcal{B}(d)$ be a disc with radius d and the center at the origin, then the average number of mobiles that associate themselves with MBS i is

$$\kappa_i = \lim_{d\to\infty} \mathbb{E} \sum_{y\in\Phi_M\bigcap\mathcal{B}(d)} \mathbf{1}\left(\frac{L(x_i,y)^{-\alpha}}{\max_{x_j\in\Phi_B/x_i} L(x_j,y)^{-\alpha}} > 1\right).$$

Applying Campbell's Theorem [45], $\kappa_i$reduces to:

$$\begin{aligned}(2\pi\lambda_M)^{-1}\kappa_i &= \lim_{d\to\infty}\int_0^d \mathbb{E}\left[\mathbf{1}\left(r^{-\alpha} > \max_{x_j\in\Phi_B/x_i}\|x_j\|^{-\alpha}\right)\right] r\,dr \\ &= \lim_{d\to\infty}\int_0^d \mathbb{E}\left[\prod_{x_j\in\Phi_B/x_i}\mathbf{1}\left(r^{-\alpha}>\|x_j\|^{-\alpha}\right)\right] r\,dr \\ &= \lim_{d\to\infty}\int_0^d \mathbb{E}\left[e^{\sum\limits_{x_j\in\Phi_B/x_i}\ln\mathbf{1}\left(r^{-\alpha}>\|x_j\|^{-\alpha}\right)}\right] r\,dr.\end{aligned} \tag{24}$$

Noticing that for given $r < d < \infty$ the function $\Sigma(r) = \sum\limits_{x_j\in\Phi_B/x_i} \ln\mathbf{1}(r^{-\alpha} > \|x_j\|^{-\alpha})$, satisfies the necessary and sufficient conditions of Campbell's Theorem, i.e., $\int_0^\infty \min\{1, |\ln\mathbf{1}(r^{-\alpha} > x^{-\alpha})|\}x\,dx = \int_0^r x\,dx < \infty$. Adopting Campbell's Theorem, there then holds

$$\begin{aligned}\kappa_i &= 2\pi\lambda_M\int_0^\infty e^{-\lambda_B\int\limits_{\mathbb{R}^2}\left[1-e^{\ln\mathbf{1}\left(r^{-\alpha}>z^{-\alpha}\right)}\right]dz} r\,dr \\ &= 2\pi\lambda_M\int_0^\infty e^{-2\pi\lambda_B\int_0^r z\,dz} r\,dr = 2\pi\lambda_M\int_0^\infty e^{-\pi\lambda_B r^2} r\,dr.\end{aligned} \tag{25}$$

By straightforward integration, it is easy to verify that $\kappa_i = \kappa = \lambda_M/\lambda_B$.

APPENDIX II

Proof of Proposition 1: The proof is similar to Theorem 1, so we briefly present necessary steps. Mobile y will connect to MBS i if the observed pilot strength is the strongest among all measured pilots, i.e., $P_T^C H_{x_iy}^{CC} L(x_i,y)^{-\alpha} > \max_{x_j\in\Phi_B/x_i} P_T^C H_{x_jy}^{CC} L(x_j,y)^{-\alpha}$. Let κ_i be

the mean value of the number of MUs associated with MBS i, then κ_i is obtained as

$$\begin{aligned}
&2\pi\lambda_M \int_0^\infty \mathbb{E}\left[\mathbf{1}\left(H_{x_i}^{CC} r^{-\alpha} > \max_{x_j\in\Phi_B/x_i} H_{x_j}^{CC}\|x_j\|^{-\alpha}\right)\right] r\,dr \\
&= 2\pi\lambda_M \int_0^\infty e^{-\pi\lambda_B \mathbb{E}_H \int_0^\infty \mathbb{P}\{H' > Hr^{-\alpha} z^{\alpha}\} z dz} r\,dr \\
&= 2\pi\lambda_M \int_0^\infty e^{-\pi\lambda_B \mathbb{E}_H \int_0^\infty f(H')dH' \int_0^{r(H'/H)^{\frac{1}{\alpha}}} z dz} r\,dr \\
&= 2\pi\lambda_M \int_0^\infty e^{-\pi\lambda_B \mathbb{E}_H\left[H^{-\frac{2}{\alpha}}\right]\mathbb{E}_H\left[H'^{\frac{2}{\alpha}}\right] r^2} r\,dr, \qquad (26)
\end{aligned}$$

which proves the proposition by recalling the Rayleigh assumption.

APPENDIX III

Proof of Lemma 2: We have $\mathbb{P}\{\|X_i\| \geq x | i = \arg\max_{x_j\in\Phi_B} H_{x_j}^{CC}\|x_j\|^{-\alpha}\} = \frac{2\pi\int_x^\infty e^{-\pi\lambda_B \mathbb{E}_H[H^{-\frac{2}{\alpha}}]\mathbb{E}_H[H'^{\frac{2}{\alpha}}]z^2} z dz}{\mathbb{P}\{i=\arg\max_{x_j\in\Phi_B}\|x_j\|^{-\alpha}\}}$, which is

$$2\pi\lambda_B \mathbb{E}_H\left[H^{-\frac{2}{\alpha}}\right]\mathbb{E}_H\left[H^{\frac{2}{\alpha}}\right] \frac{e^{-2\pi\lambda_B \mathbb{E}_H\left[H^{-\frac{2}{\alpha}}\right]\mathbb{E}_H\left[H^{\frac{2}{\alpha}}\right] x^2}}{2\pi\lambda_B \mathbb{E}_H\left[H^{-\frac{2}{\alpha}}\right]\mathbb{E}_H\left[H^{\frac{2}{\alpha}}\right]} \qquad (27)$$

since $\mathbb{P}\{i = \arg\max_{x_j\in\Phi_B}|x_j|^{-\alpha}\} = 2\pi\lambda_B \mathbb{E}_H[H^{-\frac{2}{\alpha}}]\mathbb{E}_H[H^{\frac{2}{\alpha}}]$. Fading is Rayleigh that proves the lemma.

APPENDIX IV

Proof of Theorem 2: Noting the definition of SINR given in (5), we proceed as:

$$P_c^C = \mathbb{E}_x \sum_{n=0}^\infty e^{-\kappa}\frac{\kappa^n}{n!}\mathbb{P}\left\{\frac{1}{n+1}\frac{P_T^C H_{xy_0}^{CC}\|x\|^{-\alpha}}{I_{C\to C}^0 + I_{D\to C}^0 + \sigma^2} > \beta^C\right\}.$$

The inside probability expression can be evaluated as

$$\begin{aligned}
&\mathbb{P}\left\{\frac{\frac{P_T^C}{n+1}H_{xy_0}^{CC}\|x\|^{-\alpha}}{I_{C\to C}^0 + I_{D\to C}^0 + \sigma^2} > 1 | I_{D\to C}^0 > Q\right\}\mathbb{P}\left\{I_{D\to C}^0 > Q\right\} \\
&\quad + \mathbb{P}\left\{\frac{\frac{1}{\beta^C}\frac{P_T^C}{n+1}H_{xy_0}^{CC}\|x\|^{-\alpha}}{I_{C\to C}^0 + I_{D\to C}^0 + \sigma^2} > 1 | I_{D\to C}^0 \leq Q\right\}\mathbb{P}\left\{I_{D\to C}^0 \leq Q\right\}. \qquad (28)
\end{aligned}$$

Due to the spectrum sharing regulation we know that $\mathbb{P}\{I_{D\to C}^0 > Q\} \leq \zeta$. On the other hand, $\mathbb{P}\{I_{D\to C}^0 \leq Q\} \leq 1$. Hence, (28) may be upper-bounded via

$$\begin{aligned}
&\zeta\mathbb{P}\left\{\frac{\frac{P_T^C}{n+1}H_{xy_0}^{CC}\|x\|^{-\alpha}}{I_{C\to C}^0 + I_{D\to C}^0 + \sigma^2} > \beta^C | I_{D\to C}^0 > Q\right\} \\
&\quad + \mathbb{P}\left\{\frac{1}{n+1}\frac{P_T^C H_{xy_0}^{CC}\|x\|^{-\alpha}}{I_{C\to C}^0 + I_{D\to C}^0 + \sigma^2} > \beta^C | I_{D\to C}^0 \leq Q\right\}. \qquad (29)
\end{aligned}$$

On the other hand, when $I_{D\to C}^0 > Q$ we may suggest that

$$\begin{aligned}
&\mathbb{P}\left\{\frac{1}{n+1}\frac{P_T^C H_{xy_0}^{CC}\|x\|^{-\alpha}}{I_{C\to C}^0 + I_{D\to C}^0 + \sigma^2} > \beta^C\right\} \\
&\qquad \leq \mathbb{P}\left\{\frac{1}{n+1}\frac{P_T^C H_{xy_0}^{CC}\|x\|^{-\alpha}}{I_{C\to C}^0 + Q + \sigma^2} > \beta^C\right\}. \qquad (30)
\end{aligned}$$

Also, if $I_{D\to C}^0 \leq Q$ we have

$$\begin{aligned}
&\mathbb{P}\left\{\frac{1}{n+1}\frac{P_T^C H_{xy_0}^{CC}\|x\|^{-\alpha}}{I_{C\to C}^0 + I_{D\to C}^0 + \sigma^2} > \beta^C\right\} \\
&\qquad \leq \mathbb{P}\left\{\frac{1}{n+1}\frac{P_T^C H_{xy_0}^{CC}\|x\|^{-\alpha}}{I_{C\to C}^0 + \sigma^2} > \beta^C\right\}. \qquad (31)
\end{aligned}$$

Regarding these two conditional probabilities, we can upper-bound the coverage probability as:

$$\begin{aligned}
P_c^C &\leq \mathbb{E}_x \sum_{n=0}^\infty e^{-\kappa}\frac{\kappa^n}{n!}\left[\zeta\mathbb{P}\left\{\frac{1}{n+1}\frac{P_T^C H_{xy_0}^{CC}\|x\|^{-\alpha}}{I_{C\to C}^0 + Q + \sigma^2} > \beta^C\right\}\right. \\
&\qquad \left. + \mathbb{P}\left\{\frac{1}{n+1}\frac{P_T^C H_{xy_0}^{CC}\|x\|^{-\alpha}}{I_{C\to C}^0 + \sigma^2} > \beta^C\right\}\right] \qquad (32) \\
&= \sum_{n=0}^\infty \frac{\zeta e^{-\kappa}\kappa^n}{n!}\mathbb{E}_x\mathbb{P}\left\{\frac{H_{xy_0}^{CC}}{I_{C\to C}^0 + Q + \sigma^2} > -\frac{\beta^C(n+1)}{P_T^C\|x\|^{-\alpha}}\right\} \\
&\quad + e^{-\kappa}\sum_{n=0}^\infty \frac{\kappa^n}{n!}\mathbb{E}_x\mathbb{P}\left\{\frac{H_{xy_0}^{CC}}{I_{C\to C}^0 + \sigma^2} > \frac{\beta^C(n+1)}{P_T^C\|x\|^{-\alpha}}\right\}. \qquad (33)
\end{aligned}$$

Let's first focus on (32). Since channel power gains are exponentially distributed, we may suggest

$$\begin{aligned}
&\mathbb{E}_x\mathbb{P}\left\{\frac{H_{xy_0}^{CC}}{I_{C\to C}^0 + Q + \sigma^2} > \frac{\beta^C(n+1)}{P_T^C\|x\|^{-\alpha}}\right\} \\
&\qquad = \mathbb{E}_x\mathcal{L}_{I_{C\to C}^0}\left(\frac{\beta^C(n+1)}{P_T^C\|x\|^{-\alpha}}\right)e^{-\frac{\beta^C(n+1)}{P_T^C\|x\|^{-\alpha}}(Q+\sigma^2)}, \qquad (34)
\end{aligned}$$

where $\mathcal{L}_{I_{C\to C}^0}(.)$ is the Laplace transform of $I_{C\to C}^0$. By definition, Laplace transform is

$$\begin{aligned}
\mathcal{L}_{I_{C\to C}^0}(s) &= \mathbb{E}e^{-sI_{C\to C}^0} \\
&= \mathbb{E}_{\Phi_B}\mathbb{E}_{\{N_j>0\}}\prod_{x_j\in\hat{\Phi}_B} e^{-s\frac{P_T^C}{N_j}H_{x_j y_0}^{CC}\|x_j\|^{-\alpha}\mathbf{1}\left(\|x_j\|^{-\alpha} < \|x\|^{-\alpha}\right)}. \qquad (35)
\end{aligned}$$

Note that $\{N_j\}$ are independent and identical random variables. Thus, $\mathcal{L}_{I^0_{C\to C}}(s)$ is

$$\begin{aligned}&\mathbb{E}_{\Phi_B}\prod_{x_j\in\hat{\Phi}_B}\mathbb{E}_{N_j>0}e^{-s\frac{P_T^C}{N_j}H^{CC}_{x_jy_0}\|x_j\|^{-\alpha}\mathbf{1}\left(\|x_j\|^{-\alpha}<\|x\|^{-\alpha}\right)}\\&=\exp\left(-2\pi\hat{\lambda}_B\int\limits_{r>\|x\|}\mathbb{E}_{N>0}\frac{s\frac{P_T^C}{N}r^{-\alpha}}{1+s\frac{P_T^C}{N}r^{-\alpha}}r\,dr\right)\\&=\exp\left(-\pi\hat{\lambda}_B\left(sP_T^C\right)^{\frac{2}{\alpha}}\int\limits_{r>\left(sP_T^C\right)^{-\frac{2}{\alpha}}\|x\|^2}\mathbb{E}_{N>0}\frac{1}{1+Nr^{\frac{\alpha}{2}}}dr\right).\end{aligned}\tag{36}$$

Then $\mathcal{L}_{I^0_{C\to C}}(\frac{\beta^C(n+1)}{P_T^C\|x\|^{-\alpha}})$ is

$$e^{-\pi\hat{\lambda}_B\left(\beta^C(n+1)\right)^{\frac{2}{\alpha}}F\left(\left(\beta^C(n+1)\right)^{-\frac{2}{\alpha}},\frac{\alpha}{2}\right)\|x\|^2}\tag{37}$$

where

$$F\left(\left(\beta^C(n+1)\right)^{-\frac{2}{\alpha}},\frac{\alpha}{2}\right)=\int\limits_{r>\left(\beta^C(n+1)\right)^{-\frac{2}{\alpha}}}\mathbb{E}_{N>0}\frac{1}{1+Nr^{\frac{\alpha}{2}}}dr.$$

As a result, noticing the Lemma 1 one can show that (34) reduces to

$$2\pi\lambda_B\int\limits_0^\infty e^{-\pi\hat{\lambda}_B\left(\beta^C(n+1)\right)^{\frac{2}{\alpha}}F\left(\left(\beta^C(n+1)\right)^{-\frac{2}{\alpha}},\frac{\alpha}{2}\right)x^2}\times e^{-\frac{\beta^C(n+1)x^\alpha(Q+\sigma^2)}{P_T^C}}e^{-\pi\lambda_Bx^2}x\,dx.\tag{38}$$

It is straightforward to show that $\mathbb{E}_x\mathbb{P}\{\frac{H^{CC}_{xy_0}}{I^0_{C\to C}+\sigma^2}>\frac{\beta^C(n+1)}{P_T^C\|x\|^{-\alpha}}\}$ is

$$2\pi\lambda_B\int\limits_0^\infty e^{-\frac{\beta^C(n+1)x^\alpha}{P_T^C}\sigma^2-\pi\hat{\lambda}_B\left(\beta^C(n+1)\right)^{\frac{2}{\alpha}}F\left(\left(\beta^C(n+1)\right)^{-\frac{2}{\alpha}},\frac{\alpha}{2}\right)x^2}\times e^{-\pi\lambda_Bx^2}x\,dx.\tag{39}$$

Substituting (38) and (39) in (33), the theorem follows.

Appendix V

Proof of Theorem 3: Here we only evaluate (32) in Appendix V. Straightforward manipulation indicates that

$$\begin{aligned}&\mathbb{P}\left\{\frac{H^{CC}_{xy_0}}{I^0_{C\to C}[w]+Q+\sigma^2}>\frac{\beta^C(n+1)}{P_T^C\|x\|^{-\alpha}}\right\}\\&=\mathbb{P}\left\{\frac{1}{H^{CC}_{xy_0}}I^0_{C\to C}[w]+\frac{Q+\sigma^2}{H^{CC}_{xy_0}}<\frac{P_T^C\|x\|^{-\alpha}}{\beta^C(n+1)}\right\}\\&=\mathbb{P}\left\{\sum_{x_j\in\hat{\Phi}_B[w]}\frac{H^{CC}_{x_jy_0}}{H^{CC}_{xy_0}}\frac{P_T^C\|x_j\|^{-\alpha}}{N_j}\mathbf{1}\left(\frac{H^{CC}_{x_jy_0}\|x_j\|^{-\alpha}}{H^{CC}_{xy_0}\|x\|^{-\alpha}}<1\right)\right.\\&\qquad\left.+\frac{Q+\sigma^2}{H^{CC}_{xy_0}}\le\frac{P_T^C\|x\|^{-\alpha}}{\beta^C(n+1)}\right\}.\end{aligned}\tag{40}$$

The evaluation of this probability is complicated even when $Q=\sigma^2=0$. This is mainly because of the term $\mathbf{1}(H^{CC}_{x_jy_0}\|x_j\|^{-\alpha}<H^{CC}_{xy_0}\|x\|^{-\alpha})$. We derive an upper-bound on this probability as follows. We follow the technique introduced in [44]. Let $\Delta(x)=\frac{P_T^C|x|^{-\alpha}}{\beta^C(n+1)}$ and consider the following set that contains harmfully interfering MBSs on sub-channel w

$$\begin{aligned}\Psi_B[w]=\Bigg\{x_j\in\hat{\Phi}_B[w]:\frac{Q+\sigma^2}{H^{CC}_{xy_0}}\\+\frac{H^{CC}_{x_jy_0}}{H^{CC}_{xy_0}}\frac{P_T^C\|x_j\|^{-\alpha}}{N_j}\mathbf{1}\left(\frac{H^{CC}_{x_jy_0}\|x_j\|^{-\alpha}}{H^{CC}_{xy_0}\|x\|^{-\alpha}}<1\right)>\Delta(x)\Bigg\}.\end{aligned}\tag{41}$$

An upper-bound on (40) is $\mathbb{P}\{\Psi_B[w]=\emptyset\}=\exp(-\check{\lambda}_B[w])$ where

$$\begin{aligned}\check{\lambda}_B[w]=2\pi\hat{\lambda}_B[w]\mathbb{E}_{N>0}\int\limits_0^\infty\mathbb{P}\Bigg\{\frac{Q+\sigma^2}{V}\\+\frac{W}{V}\frac{P_T^Cr^{-\alpha}}{N}\mathbf{1}\left(Wr^{-\alpha}<V\|x\|^{-\alpha}\right)>\Delta(x)\Bigg\}r\,dr.\end{aligned}\tag{42}$$

We first evaluate the inner probability that is

$$\begin{aligned}p=&\mathbb{P}\left\{\frac{W}{V}\frac{P_T^Cr^{-\alpha}}{N}+\frac{Q+\sigma^2}{V}>\Delta(x)|\frac{Wr^{-\alpha}}{V\|x\|^{-\alpha}}<1\right\}\\&\times\mathbb{P}\left\{\frac{Wr^{-\alpha}}{V\|x\|^{-\alpha}}<1\right\}+\mathbb{P}\left\{\frac{Q+\sigma^2}{V}>\Delta(x)|\frac{Wr^{-\alpha}}{V\|x\|^{-\alpha}}\ge1\right\}\\&\times\mathbb{P}\left\{\frac{Wr^{-\alpha}}{V\|x\|^{-\alpha}}\ge1\right\}.\end{aligned}\tag{43}$$

Since this probability is too complex to evaluate, we derive a lower-bound, yielding an upper-bound of the probability (40) as:

$$p\ge\mathbb{P}\left\{V<\frac{Q+\sigma^2}{\Delta(x)},V\le W\left(\frac{\|x\|}{r}\right)^\alpha\right\}\tag{44}$$

$$+\mathbb{P}\left\{\frac{W}{V}r^{-\alpha}>\frac{N\Delta(x)}{P_T^C}|\frac{Wr^{-\alpha}}{V\|x\|^{-\alpha}}<1\right\}\mathbb{P}\left\{\frac{Wr^{-\alpha}}{V\|x\|^{-\alpha}}<1\right\}.\tag{45}$$

(45) is equal to

$$\mathbb{P}\left\{\frac{N\Delta(x)}{P_T^C}r^\alpha\le\frac{W}{V}\le r^\alpha\|x\|^{-\alpha}\right\}\mathbf{1}\left(\frac{N\Delta(x)}{P_T^C}\le\|x\|^{-\alpha}\right)$$

that is

$$\mathbf{1}\left(\frac{N\Delta(x)}{P_T^C}\le\|x\|^{-\alpha}\right)\left[\frac{1}{1+\frac{N\Delta(x)}{P_T^C}r^\alpha}-\frac{1}{1+\|x\|^{-\alpha}r^\alpha}\right]\tag{46}$$

For (44) we can show that $\mathbb{P}\{V<\frac{Q+\sigma^2}{\Delta(x)},V\le W\left(\frac{\|x\|}{r}\right)^\alpha\}$ is

$$\begin{aligned}&\mathbb{P}\left\{W\ge V\left(\frac{r}{\|x\|}\right)^\alpha|V<\frac{Q+\sigma^2}{\Delta(x)}\right\}\mathbb{P}\left\{V<\frac{Q+\sigma^2}{\Delta(x)}\right\}\\&=\frac{1-e^{-\frac{Q+\sigma^2}{\Delta(x)}}}{1+\left(\frac{r}{\|x\|}\right)^\alpha}\left[1-e^{-\frac{Q+\sigma^2}{\Delta(x)}\left(1+\left(\frac{r}{\|x\|}\right)^\alpha\right)}\right].\end{aligned}\tag{47}$$

Utilizing (46) and (47), a lower-bound on p is suggested as

$$p \geq \frac{1-e^{-\frac{Q+\sigma^2}{\Delta(x)}}}{1+\left(\frac{r}{\|x\|}\right)^{\alpha}}\left[1-e^{-\frac{Q+\sigma^2}{\Delta(x)}\left(1+\left(\frac{r}{\|x\|}\right)^{\alpha}\right)}\right] + \mathbf{1}\left(\frac{N\Delta(x)}{P_T^C} \leq \|x\|^{-\alpha}\right)\left[\frac{1}{1+\frac{N\Delta(x)}{P_T^C}r^{\alpha}} - \frac{1}{1+\|x\|^{-\alpha}r^{\alpha}}\right]. \tag{48}$$

Denote Υ_Q as

$$\Upsilon_Q = 2\pi\hat{\lambda}_B[w]\int_0^{\infty}\frac{1-e^{-\frac{(Q+\sigma^2)\beta^C(n+1)}{P_T^C}}}{1+\left(\frac{r}{\|x\|}\right)^{\alpha}} \times\left[1-e^{-\frac{(Q+\sigma^2)\beta^C(n+1)}{P_T^C}\left(1+\left(\frac{r}{\|x\|}\right)^{\alpha}\right)}\right] r\,dr$$

a lower bound on $\check{\lambda}_B[w]$ then is $\check{\lambda}_B[w] = \pi\hat{\lambda}_B[w]\|x\|^2\,\mathbb{E}_{0<N\leq\beta^C(n+1)}\left(\left[\left(\frac{\beta^C(n+1)}{N}\right)^{\frac{2}{\alpha}}-1\right]\int_0^{\infty}\frac{dr}{1+r^{\frac{\alpha}{2}}}+\Upsilon_Q\right)$. Consequently, a lower bound on the coverage probability is

$$P_c^C \leq 2\pi\lambda_B\Gamma(\alpha)e^{-\tilde{\kappa}}\sum_{n=0}^{\infty}\frac{\tilde{\kappa}^n}{n!}\int_0^{\infty}\left(\zeta e^{-\check{\lambda}_B[w]}+e^{-\check{\lambda}_B[w]+\Upsilon_Q-\Upsilon}\right) \times e^{-\pi\lambda_B\Gamma(\alpha)x^2}x\,dx, \tag{49}$$

where

$$\Upsilon = 2\pi\hat{\lambda}_B[w]\int_0^{\infty}\frac{1-e^{-\frac{\sigma^2\beta^C(n+1)}{P_T^C}}}{1+\left(\frac{r}{\|x\|}\right)^{\alpha}} \times\left[1-e^{-\frac{\sigma^2\beta^C(n+1)}{P_T^C}\left(1+\left(\frac{r}{\|x\|}\right)^{\alpha}\right)}\right] r\,dr.$$

APPENDIX VI

Proof of Proposition 2: Applying near-field approximation [44] and assuming Rayleigh fading, we have

$$\begin{aligned}\lambda_O^D[w] &= \lambda_D[w]\mathbb{P}\{I^0_{C\to D_t}[w]\leq\sigma^2\varepsilon^D_{th}\}\\ &= \lambda_D[w]\mathbb{P}\left\{\sum_{x_i\in\hat{\Phi}_B[w]}\frac{P_T^C H^{CD}_{x_i z_0}}{N_i L(x_i,z_0)^{\alpha}}\leq\sigma^2\varepsilon^D_{th}\right\}\\ &\approx \lambda_D[w]\mathbb{P}\left\{\left\{x_i\in\hat{\Phi}_B[w]:\frac{P_T^C H^{CD}_{x_i z_0}}{N_i L(x_i,z_0)^{\alpha}}>\sigma^2\varepsilon^D_{th}\right\}=\emptyset\right\}\\ &= \lambda_D[w]e^{-2\pi\hat{\lambda}_B[w]\mathbb{E}_{N>0}\int_0^{\infty}e^{-N\frac{\sigma^2\varepsilon^D_{th}}{P_T^C}x^{\alpha}}x\,dx}\\ &= \lambda_D[w]e^{-\pi\hat{\lambda}_B[w]\left(\frac{P_T^C}{\sigma^2\varepsilon^D_{th}}\right)^{\frac{2}{\alpha}}\Gamma\left(1+\frac{2}{\alpha}\right)e^{-\kappa}\sum_{n=1}^{\infty}\frac{\kappa^n}{n!}n^{-\frac{2}{\alpha}}}.\end{aligned} \tag{50}$$

APPENDIX VII

Proof of Theorem 4: To derive the isolation probability, we first obtain the mean value of a TD's neighbors $\delta[w]$. Among the devices that stay silent, with probability $1-a_D[w]$ on each sub-channel, those that can receive detectable information from a given TD l are its neighbors [33]. Then,

$$\begin{aligned}\delta[w] &= \mathbb{E}\sum_{z_l\in\Psi_R^D[w]}\mathbf{1}\left(\mathrm{SINR}_0^D\geq\beta^D\right)\\ &= \lambda_R^D[w]\int_{\mathbb{R}^2}\mathbb{P}\left\{\frac{P_O^D H^{DD}_{zz_0}\|z\|^{-\alpha}}{I^0_{C\to D}[w]+\sigma^2}\geq\beta^D\right\}\mathbb{P}\{\text{Overlay}\}\,dz\\ &\quad+\lambda_R^D[w]\int_{\mathbb{R}^2}\mathbb{P}\left\{\frac{P_O^D H^{DD}_{zz_0}\|z\|^{-\alpha}}{I^0_{C\to D}[w]+\sigma^2}\geq\beta^D\right\}\mathbb{P}\{\text{Underlay}\}\,dz.\end{aligned} \tag{51}$$

We only need to substitute following formulas

$$\begin{aligned}\mathbb{P}\{\text{Underlay}\} &= \mathbb{P}\{I^0_{C\to D}>\sigma^2\varepsilon^D_{th}\}\\ &\approx 1-e^{-\pi\hat{\lambda}_B[w]\left(\frac{P_T^C}{\sigma^2\varepsilon^D_{th}}\right)^{\frac{2}{\alpha}}\Gamma\left(1+\frac{2}{\alpha}\right)e^{-\kappa}\sum_{n=1}^{\infty}\frac{\kappa^n}{n!}n^{-\frac{2}{\alpha}}},\end{aligned} \tag{52}$$

$$\begin{aligned}\mathbb{P}\{\text{Overlay}\} &= \mathbb{P}\{I^0_{C\to D}\leq\sigma^2\varepsilon^D_{th}\}\\ &\approx e^{-\pi\hat{\lambda}_B[w]\left(\frac{P_T^C}{\sigma^2\varepsilon^D_{th}}\right)^{\frac{2}{\alpha}}\Gamma\left(1+\frac{2}{\alpha}\right)e^{-\kappa}\sum_{n=1}^{\infty}\frac{\kappa^n}{n!}n^{-\frac{2}{\alpha}}},\end{aligned} \tag{53}$$

$$\begin{aligned}&\mathbb{P}\left\{\frac{P_O^D H^{DD}_{zz_0}\|z\|^{-\alpha}}{I^0_{C\to D}[w]+\sigma^2}\geq\beta^D\right\}\\ &= e^{-\frac{\beta^D\|z\|^{\alpha}}{P_O^D}\sigma^2}e^{-\pi\hat{\lambda}_B[w]\left(\frac{\beta^D P_T^C}{P_O^D}\right)^{\frac{2}{\alpha}}\|z\|^2\Gamma\left(1+\frac{2}{\alpha}\right)e^{-\kappa}\sum_{n=1}^{\infty}\frac{\kappa^n}{n!}n^{-\frac{2}{\alpha}}},\end{aligned} \tag{54}$$

$$\begin{aligned}&\mathbb{P}\left\{\frac{P_O^D H^{DD}_{zz_0}\|z\|^{-\alpha}}{I^0_{C\to D}[w]+\sigma^2}\geq\beta^D\right\}\\ &= e^{-\frac{\beta^D\|z\|^{\alpha}}{P_U^D}\sigma^2}e^{-\pi\hat{\lambda}_B[w]\left(\frac{\beta^D P_T^C}{P_U^D}\right)^{\frac{2}{\alpha}}\|z\|^2\Gamma\left(1+\frac{2}{\alpha}\right)e^{-\kappa}\sum_{n=1}^{\infty}\frac{\kappa^n}{n!}n^{-\frac{2}{\alpha}}}.\end{aligned} \tag{55}$$

APPENDIX VIII

Proof of Theorem 5: The necessary condition for devices that are communicating on sub-channel w to percolate is $[w]=\frac{1}{a_D[w]}$ since $1-a_D[w]$ amounts to the failure probability in the site-percolation model [33], [34]. Noting the obtained expression for $\delta[w]$ in Theorem 4, this necessary condition solves the equation $\delta[w]=\frac{1-a_D[w]}{a_D[w]}(T_U[w]+T_O[w])=\frac{1}{a_D[w]}$ for $a_D[w]$. Elementary calculus then proves the result.

REFERENCES

[1] L. Lei, Z. Zhong, C. Lin, and X. Shen, "Operator controlled device-to-device communications in LTE-Advanced networks," *IEEE Wireless Commun.*, vol. 19, no. 3, pp. 96–104, Jun. 2012.

[2] G. Fodor *et al.*, "Design aspects of network assisted device-to-device communications," *IEEE Commun. Mag.*, vol. 50, no. 3, pp. 170–177, Mar. 2012.

[3] C. H. Yu, K. Doppler, C. B. Riberio, and O. Trikkonen, "Resource sharing optimization for device-to-device communication underlying cellular networks," *IEEE Trans. Wireless Commun.*, vol. 10, no. 8, pp. 2752–2763, Aug. 2011.

[4] F. Pantisano, M. Bennis, W. Saad, and M. Debbah, "Spectrum leasing as an incentive towards uplink macrocell and femtocell cooperation," *IEEE J. Sel. Areas Commun.*, vol. 30, no. 3, pp. 617–630, Apr. 2012.

[5] S. Haykin, "Cognitive radio: Brain-empowered wireless communications," *IEEE J. Sel. Areas Commun.*, vol. 23, no. 2, pp. 201–220, Feb. 2005.

[6] D. Niyato, L. Xiao, and P. Wang, "Machine-to-machine communications for home energy management system in smart grid," *IEEE Commun. Mag.*, vol. 49, no. 4, pp. 53–59, Apr. 2011.

[7] S. Y. Lien, T. H. Liau, C. Y. Kao, and K. C. Chen, "Cooperative access class barring for machine-to-machine communications," *IEEE Trans. Wireless Commun.*, vol. 11, no. 1, pp. 27–32, Jan. 2012.

[8] S. Y. Lien, K. C. Chen, and Y. Lin, "Toward ubiquitous massive access in 3GPP machine-to-machine communications," *IEEE Commun. Mag.*, vol. 49, no. 4, pp. 66–74, Apr. 2011.

[9] J. Zhang, L. Shan, and Y. Yang, "Mobile cellular networks and wireless sensor networks: Toward convergence," *IEEE Commun. Mag.*, vol. 50, no. 3, pp. 164–169, Mar. 2012.

[10] H. Min, J. Lee, S. Park, and D. Hong, "Capacity enhancement using an interference limited area for device-to-device uplink underlaying cellular networks," *IEEE Trans. Wireless Commun.*, vol. 10, no. 12, pp. 3995–4000, Dec. 2011.

[11] H. Min, W. Seo, J. Lee, S. Park, and D. Hong, "Reliability improvement using receive mode selection in the device-to-device uplink period underlaying cellular networks," *IEEE Trans. Wireless Commun.*, vol. 10, no. 2, pp. 413–418, Feb. 2011.

[12] K. Doppler, M. Rinne, C. Wijting, C. B. Riberio, and K. Hugl, "Device-to-device communication as an underlay to LTE-Advanced networks," *IEEE Commun. Mag.*, vol. 47, no. 12, pp. 42–49, Dec. 2009.

[13] M. Jung, K. Hwang, and S. Choi, "Joint mode selection and power allocation scheme for power-efficient device-to-device (D2D) communication," in *Proc. IEEE VTC-spring*, May 2012, pp. 1–5.

[14] H. Wu, C. Qiao, S. De, and O. Tonguz, "Integrated cellular and ad hoc relaying systems: iCAR," *IEEE J. Sel. Areas Commun.*, vol. 19, no. 10, pp. 2105–2115, Oct. 2001.

[15] K. Huang, V. K. N. Lan, and Y. Chen, "Spectrum sharing between cellular and ad hoc networks: Transmission–capacity trade-off," *IEEE J. Sel. Areas Commun.*, vol. 27, no. 7, pp. 1256–1267, Sep. 2009.

[16] B. Kaufman, J. Lilleberg, and B. Aazhang, "Spectrum sharing scheme between cellular users and ad-hoc device-to-device users," *IEEE Trans. Wireless Commun.*, vol. 12, no. 3, pp. 1038–1049, Mar. 2013.

[17] B. Kaufman, B. Aazhang, and J. Lilleberg, "Interference aware link discovery for device to device communication," in *Proc. 43rd Asilomar Conf. Signals, Syst. Comput.*, Nov. 2009, pp. 297–301.

[18] M. C. Erturk, S. Mukherjee, H. Ishii, and H. Arslan, "Distributions of transmit power and SINR in device-to-device networks," *IEEE Commun. Lett.*, vol. 17, no. 2, pp. 273–276, Feb. 2013.

[19] J. Lee, J. G. Andrew, and D. Hong, "Spectrum-sharing transmission capacity," *IEEE Trans. Wireless Commun.*, vol. 10, no. 9, pp. 3053–3063, Sep. 2011.

[20] W. C. Cheung, T. Q. S. Quek, and M. Kountouris, "Throughput optimization, spectrum allocation, access control in two-tier femtocell networks," *IEEE J. Sel. Areas Commun.*, vol. 30, no. 3, pp. 561–574, Apr. 2012.

[21] E. Axell, G. Leus, E. G. Larsson, and H. V. Poor, "Spectrum sensing for cognitive radio: State-of-the-art and recent advances," *IEEE Signal Process. Mag.*, vol. 29, no. 3, pp. 101–116, May 2012.

[22] M. G. Khoshkholgh, K. Navaie, and H. Yanikomeroglu, "Outage performance of the primary service in spectrum sharing networks," *IEEE Trans. Mobile Comput.*, vol. 12, no. 10, pp. 1955–1971, Aug. 2013.

[23] Q. Zhao and B. Sadler, "A survey of dynamic spectrum access," *IEEE Signal Process. Mag.*, vol. 24, no. 3, pp. 79–89, May 2007.

[24] N. Mokari, K. Navaie, and M. G. Khoshkholgh, "Downlink radio resource allocation in OFDMA spectrum sharing environment with partial channel state information," *IEEE Trans. Wireless Commun.*, vol. 10, no. 10, pp. 3482–3495, Oct. 2011.

[25] M. G. Khoshkholgh, N. Mokari, and K. G. Shin, "Ergodic sum capacity of spectrum-sharing multiple access with collision metric," *IEEE J. Sel. Areas Commun.*, vol. 31, no. 11, pp. 2528–2540, Nov. 2013.

[26] A. Ghasemi and E. S. Sousa, "Interference aggregation in spectrum-sensing cognitive wireless networks," *IEEE J. Sel. Topics Signal Process.*, vol. 2, no. 1, pp. 41–56, Feb. 2008.

[27] A. D. D. Garcia, C. N. Hadjicostis, and N. H. Vaidya, "Resilient networked control of distributed energy resources," *IEEE J. Sel. Areas Commun.*, vol. 30, no. 6, pp. 1137–1148, Jul. 2012.

[28] H. Li, L. Lai, and H. V. Poor, "Multicast routing for decentralized control of cyber physical systems with an application in smart grid," *IEEE J. Sel. Areas Commun.*, vol. 30, no. 6, pp. 1097–1107, Jul. 2012.

[29] A. H. Mohsenian-Rad, V. W. S. Wong, J. Jatskevich, R. Schober, and A. Leon-Garcia, "Autonomous demand-side management based on game-theoretic energy consumption scheduling for the future smart grid," *IEEE Trans. Smart Grid*, vol. 1, no. 3, pp. 320–331, Dec. 2010.

[30] J. G. Andrews, F. Baccelli, and R. K. Ganti, "A tractable approach to coverage and rate in cellular networks," *IEEE Trans. Commun.*, vol. 59, no. 11, pp. 3122–3134, Nov 2011.

[31] H. S. Jo, Y. J. Sang, P. Xia, and J. G. Andrews, "Heterogeneous cellular networks with flexible cell association: A comprehensive downlink SINR analysis," *IEEE Trans. Wireless Commun.*, vol. 11, no. 10, pp. 3484–3495, Oct. 2012.

[32] X. Lin, J. G. Andrews, and A. Ghosh, "Modeling, analysis and design for carrier aggregation in heterogeneous cellular networks," *IEEE Trans. Commun.*, vol. 61, no. 9, pp. 4002–4015, Sep. 2013.

[33] W. C. Ao, S. M. Cheng, and K. C. Chen, "Connectivity of multiple cooperative cognitive radio ad hoc networks," *IEEE J. Sel. Areas Commun.*, vol. 30, no. 2, pp. 263–270, Feb. 2012.

[34] W. C. Ao and K. C. Chen, "Cognitive radio-enabled network-based cooperation: From a connectivity perspective," *IEEE J. Sel. Areas Commun.*, vol. 30, no. 10, pp. 1969–1982, Nov. 2012.

[35] M. Haenggi, J. G. Andrews, F. Baccelli, O. Dousse, and M. Franceschetti, "Stochastic geometry and random graphs for the analysis and design of wireless networks," *IEEE J. Sel. Areas. Commun.*, vol. 27, no. 7, pp. 1029–1046, Sep. 2009.

[36] F. Baccelli, B. Baszczyszyn, and P. Muhlethaler, "Stochastic analysis of spatial and opportunistic ALOHA," *IEEE J. Sel. Areas. Commun.*, vol. 27, no. 7, pp. 1105–1119, Sep. 2009.

[37] M. G. Khoshkholgh, K. Navaie, and H. Yanikomeroglu, "Access strategies for spectrum sharing in fading environment: Overlay, underlay, mixed," *IEEE Trans. Mobile Comput.*, vol. 9, no. 12, pp. 1780–1793, Dec. 2010.

[38] M. G. Khoshkholgh, K. Navaie, and H. Yanikomeroglu, "Optimal design of the spectrum sensing parameters in the overlay spectrum sharing," *IEEE Trans. Mobile Comput.*, vol. 13, no. 9, pp. 2071–2085, Sep. 2014.

[39] X. Y. H. Kim, G. de Veciana, and M. Venkatachalam, "Distributed α-optimal user association and cell load balancing in wireless networks," *IEEE/ACM Trans. Netw.*, vol. 59, no. 11, pp. 3122–3134, Nov. 2011.

[40] K. Son, H. Kim, Y. Yi, and B. Krishnamachari, "Base station operation and user association mechanisms for energy–delay tradeoffs in green cellular networks," *IEEE J. Sel. Areas Commun.*, vol. 29, no. 8, pp. 1525–1536, Sep. 2011.

[41] F. Baccelli and B. Blaszczyszyn, "Stochastic geometry and wireless networks, Vol. I Theory," *Found. Trends Netw.*, vol. 3, no. 3/4, Mar. 2009. [Online]. Available: http://hal.inria.fr/docs/00/43/87/68/PDF/FnT1.pdf

[42] D. Stoyan, W. Kendall, and J. Mecke, *Stochastic Geometry and Its Applications*. Chichester, U.K.: Wiley, 1995.

[43] F. Baccelli, C. Gloaguen, and S. Zuyev, "Superposition of planar Voronoi tessellations," *Stochastic Models*, vol. 16, no. 1, pp. 69–98, Mar. 2000.

[44] S. P. Weber, J. G. Andrews, and N. Jindal, "The effect of fading, channel inversion, threshold scheduling on ad hoc networks," *IEEE Trans. Inf. Theory*, vol. 53, no. 11, pp. 4127–4149, Nov. 2007.

[45] J. F. C. Kingman, *Poisson Processes*. London, U.K.: Oxford Univ. Press, 1993.

Mohammad G. Khoshkholgh received the B.Sc. degree in electrical engineering from the University of Isfahan, Isfahan, Iran, in 2006 and the M.Sc. degree in electrical engineering from Tarbiat Modares University, Tehran, Iran, in 2008. He was with the Wireless Innovation Laboratory, Tarbiat Modares University, from 2008 until 2012. From February 2012 to February 2014, he was with Simula Research Laboratory, Oslo, Norway, working on developing communication solutions for smart grid systems. He is now with The University of British Columbia, Vancouver, BC, Canada. His research interests are mainly in wireless communications, radio resource allocations, and spectrum sharing.

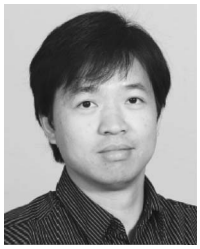

Yan Zhang (SM'10) received the Ph.D. degree from Nanyang Technological University, Singapore. Since August 2006, he has been with Simula Research Laboratory, Oslo, Norway, where he is currently a Senior Research Scientist. He is an Adjunct Associate Professor at the University of Oslo, Oslo. He is a Regional Editor, Associate Editor, on the Editorial Board, or Guest Editor of a number of international journals. His research interests include wireless networks and smart grid communications.

Kwang-Cheng Chen (M'89–SM'93–F'07) received the B.S. degree from National Taiwan University, Taipei, Taiwan, in 1983 and the M.S. and Ph.D. degrees from the University of Maryland, College Park, MD, USA, in 1987 and 1989, all in electrical engineering. From 1987 to 1998, he was with SSE, COMSAT, IBM Thomas J. Watson Research Center, and National Tsing Hua University, in mobile communications and networks. Since 1998, he has been with National Taiwan University, where he is the Distinguished Professor and Associate Dean in Academic Affairs for the College of Electrical Engineering and Computer Science. Dr. Chen was SKKU Fellow Professor 2012–2013. He has authored and co-authored over 250 technical papers and more than 20 granted U.S. patents. He co-edited (with R. DeMarca) the book *Mobile WiMAX* (Wiley, 2008), authored the book *Principles of Communications* (River, 2009), and co-authored (with R. Prasad) another book *Cognitive Radio Networks* (Wiley, 2009). His research interests include wireless communications and network science. He has been actively involved in the organization of various IEEE conferences as a General/TPC Chair/Co-Chair. He has served in editorships with a few IEEE journals and many international journals and has served in various positions within IEEE. He also actively participates in and has contributed essential technology to various IEEE 802, Bluetooth, and 3GPP wireless standards. He has received a number of awards, including the 2011 IEEE COMSOC WTC Recognition Award, and has co-authored a few award-winning papers published in the IEEE ComSoc journals and conferences, including 2014 IEEE Jack Neubauer Memorial Award.

Kang G. Shin (S'75–M'78–SM'83–F'92–LF'12) is the Kevin and Nancy O'Connor Professor of Computer Science at the Department of Electrical Engineering and Computer Science, University of Michigan, Ann Arbor, MI, USA.

He was a co-founder of a couple of start-ups and also licensed some of his technologies to industry. He has supervised the completion of 74 Ph.D. theses and authored/coauthored more than 800 technical articles (more than 300 of these are in archival journals), a textbook, and more than 20 patents or invention disclosures. His current research focuses on QoS-sensitive computing and networking, as well as on embedded real-time and cyber–physical systems. He was a recipient of numerous best paper awards, including the Best Paper Awards from the 2011 ACM International Conference on Mobile Computing and Networking (MobiCom'11), the 2011 IEEE International Conference on Autonomic Computing, the 2010 and 2000 USENIX Annual Technical Conferences, as well as the 2003 IEEE Communications Society William R. Bennett Prize Paper Award and the 1987 Outstanding IEEE Transactions of Automatic Control Paper Award. He was also a recipient of several institutional awards, including the Research Excellence Award in 1989, Outstanding Achievement Award in 1999, Distinguished Faculty Achievement Award in 2001, and Stephen Attwood Award in 2004 from the University of Michigan (the highest honor bestowed to Michigan Engineering faculty); a Distinguished Alumni Award of the College of Engineering, Seoul National University in 2002; 2003 IEEE RTC Technical Achievement Award; and 2006 Ho-Am Prize in Engineering (the highest honor bestowed to Korean-origin engineers).

Stein Gjessing received the Cand. Real. and Dr. Philos. degrees from the University of Oslo, Oslo, Norway, in 1975 and 1985, respectively. He is a Professor of computer science at the Department of Informatics, University of Oslo. He acted as the Head of the Department of Informatics for four years from 1987. From February 1996 to October 2001, he was the Chairman of the national research program Distributed IT-System, founded by the Research Council of Norway. His original work was in the field of programming languages and programming language semantics, particularly related to object oriented concurrent programming. He has worked with computer interconnects and computer architecture for cache coherent shared memory, with DRAM organization, with ring based LANs (IEEE Standard 802.17), and with IP fast reroute. His current research interests are transport, routing, and network resilience in Internet-like networks, sensor networks, and the smart grid.